5-2014

Analysis of Full-Scale Mechanically Stabilized Earth (MSE) Wall Using Crimped Steel Wire Reinforcement

Joshua Aaron Jensen

ANALYSIS OF FULL-SCALE MECHANICALLY STABILIZED EARTH (MSE) WALL USING CRIMPED STEEL WIRE REINFORCEMENT

by

Joshua Aaron Jensen

A thesis submitted in partial fulfillment
of the requirements for the degree

of

MASTER OF SCIENCE

in

Civil and Environmental Engineering

Approved:

_____	_____
James A. Bay Major Professor	John D. Rice Committee Member
_____	_____
Kevin P. Heaslip Committee Member	Mark R. McLellan Vice President for Research and Dean of the School of Graduate Studies

UTAH STATE UNIVERSITY
Logan, Utah

2014

ABSTRACT

Analysis of Full-Scale Mechanically Stabilized Earth (MSE) Wall

Using Crimped Steel Wire Reinforcement

by

Joshua Aaron Jensen, Master of Science

Utah State University, 2014

Major Professor: Dr. James A. Bay
Department: Civil and Environmental Engineering

Mechanically Stabilized Earth (MSE) walls have provided an effective solution to constructing retaining walls. The engineering and construction industry is continually striving to provide more cost-effective and design-efficient means to building MSE walls. Hilfiker Retaining Walls has developed a new semi-extensible metal mat reinforcement technology which does not fit into the current extensible or inextensible categories as defined by regulating authorities. The objective of this project was to construct and observe the behavior collect quantitative data for a 20-foot tall MSE wall using the prototype semi-extensible reinforcement technology. The results were compared to expected American Association of State Highway and Transportation Officials Load Reduction Factored Design values and was also compared to another case study, *Prediction of Reinforcement Loads in Reinforced Soil Walls* as conducted by Tony M. Allen, P.E., and Richard J. Bathurst, Ph. D., P. Eng. Comparing the behavior of the 20-

foot prototype MSE wall to these design regulations and case studies allowed for proper classification and will facilitate future industry design efforts.

(76 pages)

PUBLIC ABSTRACT

Analysis of Full-Scale Mechanically Stabilized Earth (MSE) Wall

Using Crimped Steel Wire Reinforcement

Joshua Aaron Jensen, Master of Science

The Civil and Environmental Engineering department at Utah State University partnered with Hilfiker Retaining Walls to study the behavior and feasibility of crimped steel wire mat reinforcements. Researchers from Utah State University organized the study and created the design for a full-scale model. Construction efforts were completed in cooperation of laborers from Utah State University, Hilfiker Retaining Walls, and Circle C Construction. The purpose of the study was to analyze the behavior and feasibility of a full-scale MSE wall using crimped steel wire mat reinforcements.

The estimated cost of the project was $53,600. The cost included the material cost of the crimped wire mat reinforcement, the preliminary research, construction efforts, data collection and analysis.

We collected data from the instruments placed during wall construction and used this information to support our findings. The study proved that crimped steel wire mat reinforcements may be a viable option to retaining wall design, and provide future benefit to construction efforts and budgets.

DEDICATION

I like to dedicate this thesis to my family, primarily to my wife and children because they are my motivation to do better in life. Then to my parents; they have always pushed me to do my best and taught me to never give up. Without them, I never could have accomplished such a feat as this. Lastly, I dedicate this thesis to God in search for all knowledge and all things that are true.

Joshua Aaron Jensen

ACKNOWLEDGMENTS

I would first like to express my many thanks to my major advisor, Dr. Jim Bay. He is an extremely intelligent man whose brain ceases to rest until the correct solution is reached. To be a part of this project with his guidance has been a priceless asset to my skills in the field of geotechnical engineering. I would also like to thank my committee members, Dr. John Rice and Dr. Kevin Heaslip, for their participation in this project. I would also like to thank Dr. Loren Anderson for his valuable input toward this project.

Many thanks are due to Ken Jewkes for his willingness to be a part of this project. His skill as a machinist and his common sense creativity to solve problems are not surpassed by many others. I appreciate the time he gave to me personally and for the tools he graciously lent to the success of this project.

I would like to thank Hilfiker Retaining Walls for the financial support to see this project through. Their innovation as a company and desire to stay ahead of the competition has done much to further the research in MSE walls. They have contributed much to the Civil Engineering Department at Utah State University and to the advancement of graduate students.

I would also like to thank all of the engineers who participated in the 2012 spring Hilfiker conference in Eureka, CA for their input on this project and for encouraging me to continue in the field of geotechnical engineering.

Joshua Aaron Jensen

CONTENTS

Page

LIST OF TABLES

LIST OF FIGURES

CHAPTER 1

INTRODUCTION, OBJECTIVES, AND ORGANIZATION

1.1 Introduction

Mechanically Stabilized Earth (MSE) walls have been a method of constructing retaining walls for many years. It is a simple method of construction which relies on minimally reinforcing a soil structure such that the reinforcement will effectively carry a portion of the resultant loads caused by the weight of the soil and any additional external forces.

Over the years engineering practice has become polarized in the methods used to reinforce a MSE wall using “inextensible material” or “extensible material”. The inextensible materials primarily consist of formed steel bars or wire mats, whereas the extensible materials can vary widely in different types of plastic polymers used. Typically the extensible materials are categorized in a single group known as geosynthetics and are formed as plastic mesh and grids or woven together as a fabric, much like a tarp.

1.2 Objectives

The focus of this project is to analyze a full scale prototype MSE wall with reinforcement material that lies somewhere between an extensible reinforcement material and an inextensible reinforcement material. The reinforcement to be tested is considered a semi-extensible product developed by Hilfiker Retaining Walls that incorporates the positive aspects of both types of reinforcement materials. This is accomplished by

crimping a few small sections of longitudinal wire in commonly used steel wire reinforcement mats. The purpose is to provide adequate yield deformation in the wire mats to achieve an active state in the wall, but to avoid the long term creep effects which often plague extensible geosynthetic reinforcements (Suncar, 2010). The purpose of achieving an active state in the wall is to lessen the effective loads in the internal design of the wall. By reducing the load applied to the reinforcement, a smaller diameter wire size may be used. This would reduce the amount of steel required to produce the wire mat reinforcements. With less material required to construct an MSE wall, MSE walls become more viable when selecting a design option. This design also has potential to lessen the amount of steel required for development length, but development length is primarily governed by external stability design rather than internal design of the reinforcement.

This project also makes comparisons between the AASHTO Load Reduction Factored Design (LRFD) method and the K-Stiffness design method. The AASHTO Allowable Stress Design (ASD) Method has been in practice for many years, but the shift to LRFD method is a rather new addition to MSE wall design. It has come under scrutiny that it does not accurately predict the behavior of MSE walls. The K-stiffness method developed in 2003 by Allen and Bathurst (Allen & Bathurst, 2003) is based on case studies and is an empirical approach to MSE wall design. The K-stiffness method is still undergoing peer review and has yet to be widely accepted.

1.3 Organization

A literature review was conducted to provide background and technical information needed to outline the rest of the thesis and occupies Chapter 2. Chapter 3 is the methods and testing portion of this thesis and covers the instrumentation and construction of the proposed MSE wall, whereas Chapter 4 presents the results of the testing. Chapter 5 compares the results observed to the expected behavior as presented by AASHTO LRFD design as well as the K-stiffness design. Chapter 6 summarizes the findings as a conclusion to the thesis.

CHAPTER 2

LITERATURE REVIEW

2.1 Background

Mechanically Stabilized Earth (MSE) walls have continually been a focus of study since their inception into standard engineering practice. The method of constructing an earth retaining structure consisting of soil and minimal reinforcement is both effective and cost efficient. The industry of MSE walls is continually striving to become more effective and cost efficient to remain competitive in the market. This increase comes by gaining a greater understanding of wall performance compared to current standard design practices and by developing new methods of soil reinforcements.

This chapter provides the background information on current design practices as dictated by the American Association of State Highway and Transportation Officials (AASHTO), as well as a relatively new design called the K-Stiffness method.

2.2 AASHTO Load Reduction Factored Design for MSE Walls

2.2.1 General

The AASHTO Load Reduction Factored Design (LRFD) for MSE walls presented in this thesis is taken from the AASHTO Bridge Design Specifications 5th edition, 2010 manual. The purpose of designing from LRFD methods rather than allowable strength design (ASD) methods is to present a design methodology focusing more on probabilistic failure modes and limit states rather than simply assuming factors of safety for calculated loads and resistances. Since the focus of the paper is to test the internal design of MSE

wall structures, only information relevant to the internal design portion of the AASHTO LRFD method will be presented.

2.2.2 Load and Resistance Factors

The loads applied to the MSE retaining wall are magnified by given load factors depending on its limit state and the resistances are reduced by given resistance factors depending on its respective limit states. A limit state check is then performed between the factored nominal loads and the reduced nominal resistances. If the reduced nominal resistances are greater than the factored nominal loads then the design is considered competent.

The internal failure modes for MSE walls are the subject to be considered in this particular project and therefore the external design for MSE walls is not presented in this literature review. It is suffice to say, the proposed MSE wall for this project was designed according to external design specifications and meets the design requirements.

Table 2.1 shows the load factors for a given type of load to be applied in the wall and in what circumstance. Table 2.2 shows the resistance factors for MSE walls, including gravity walls and semi-gravity walls.

Table 2.1 Load Factors used in MSE wall design (AASHTO, 2010)

Type of Load, Foundation Type, and Method Used to Calculate Downdrag		Load Factor	
		Maximum	Minimum
DC: Component and Attachments DC:		1.25	0.90
Strength IV Only		1.50	0.90
DD: Downdrag	Piles, a Tomlinson Method	1.40	0.25
	Piles, l Method	1.05	0.30
	Drilled Shafts, O'Neill and Reese (1999) Method	1.25	0.35
DW: Wearin Surfaces and Utilities		1.50	0.65
EH: Horizontal Earth Pressure			
Active		1.50	0.90
At-Rest		1.35	0.90
AEP for anchored walls		1.35	N/A
EL: Locked-in Construction Stresses		1.00	1.00
EV: Vertical Earth Pressure			
Overall Stability		1.00	N/A
Retaining Walls and Abutments		1.35	1.00
Rigid Buried Structure		1.30	0.90
Rigid Frames		1.35	0.90
Flexible Buried Structures:			
	Metal Box Culverts and Structural Plate Culverts with Deep Corrugations	1.50	0.90
	Thermoplastic culverts	1.30	0.90
	All others	1.95	0.90
ES: Earth Surcharge		1.50	0.75

Table 2.2 Resistance Factors for MSE wall design (AASHTO, 2010)

Mechanically Stabilized Earth Walls, Gravity Walls, and Semi-Gravity Walls		Resistance Factor
Bearing Resistance	Gravity and semi-gravity walls	0.55
	MSE walls	0.65
Sliding		1.0
Tensile resistance of metallic reinforcement and connectors	Strip Reinforcements:	
	Static Loading	0.75
	Combined static/earthquake loading	1.00
	Grid reinforcements:	
	Static Loading	0.65
	Combined static/earthquake loading	0.85
Tensile resistance of geosythetic reinforcement and connectors	Static Loading	0.90
	Combined static/earthquake loading	1.20
Pullout resistance of tensile reinforcement	Static Loading	0.90
	Combined static/earthquake loading	1.20

2.2.3 Minimum Length of Soil Reinforcement

For MSE walls it is required the reinforcement, regardless of the type of reinforcement used, should be at least 70% of the height of the wall measured from the leveling pad. This is the minimum length of the reinforcement and could be even longer if a surcharge or other external loads require a longer length of reinforcement. The commentary in the AASHTO design specifications recognizes that the value of 70% of the wall height has no theoretical value but has been more or less adopted as a standard because it has higher success rates. The commentary provides exceptions to the minimum reinforcement lengths only if the site meets specific qualifications and can be soundly defended (AASHTO, 2010).

The length of reinforcement is required to be the same throughout the height of the wall, but can vary if evidence is provided that the change can still meet external stability requirements. It is also mentioned in the commentary that the uppermost layers may be lengthened to meet pullout requirements, the lower reinforcement layers may be lengthened to meet global stability requirements, and the bottom reinforcement layers may be shortened to minimize excavation only if the wall is bearing on rock or very competent soil. It is stated that to qualify as such, the blow counts from a standard penetration test (SPT) should be greater than 50 blows per foot. If the soil meets this requirement, it can be shortened to a minimum of 40% of the wall height, but must still meet the global stability requirements (AASHTO, 2010).

2.2.4 Internal Design

The AASHTO ASD Simplified Method for MSE wall design was used for this project and the load calculations for the method will be presented in this section. The loads are calculated at two critical locations. These locations are at the connection of the reinforcement to the facing and at the locus of maximum tension. Rupture and pullout failures are calculated along the locus of maximum tension. The maximum friction angle of the reinforced soil that may be used in design is 34 degrees if no testing of the soil has been done. The friction angle may be increased up to 40 degrees if tests are performed but no increase beyond 40 degrees is permitted (AASHTO, 2010).

The maximum loads seen in the reinforcement of MSE walls are calculated by first finding the vertical stresses at the depth of the individual reinforcement layers due to the soil and then multiplied by a lateral earth pressure coefficient. Figure 2.1 shows the geometry and dimensions for the calculations of the vertical stresses behind the face of a MSE wall.

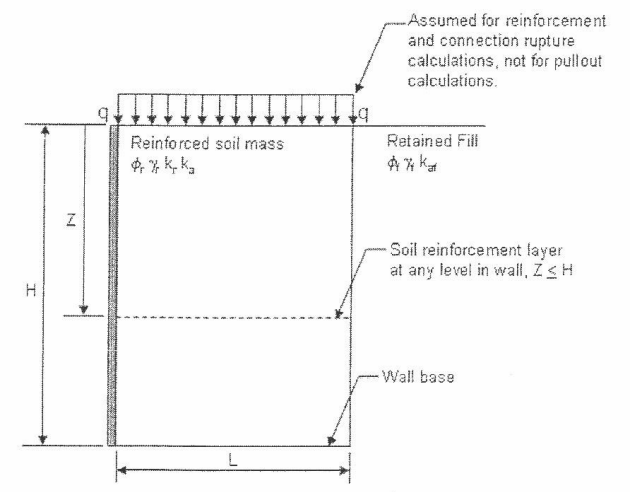

Figure 2.1 Geometry of general MSE wall design (AASHTO, 2010)

Equation 2.1 shows how the vertical stresses, σ_v, are calculated.

$$\sigma_v = \gamma_r Z + q \tag{2.1}$$

where γ_r is the unit weight of the reinforced soil mass, Z is the depth to the reinforcement layer, q is the surcharge or external loads applied at the top of the wall (AASHTO, 2010). Equation 2.2 shows the calculation of the factored horizontal stresses, σ_H, for a given vertical stress.

$$\sigma_H = \gamma_P(\sigma_v k_r) \tag{2.2}$$

where γ_P is the load factor for vertical earth pressure (EV) from table 2.1, σ_v is the vertical stress due to the reinforced soil and any applicable external loads as found from equation 2.1, and k_r is the horizontal pressure coefficient derived from Figure 2.2 (AASHTO, 2010).

The horizontal pressure coefficient, k_r, is found by multiplying the active earth pressure coefficient, k_a, by a factor found from Figure 2.2 for the given type of reinforcement used in the wall respective to its depth below the top of the wall.

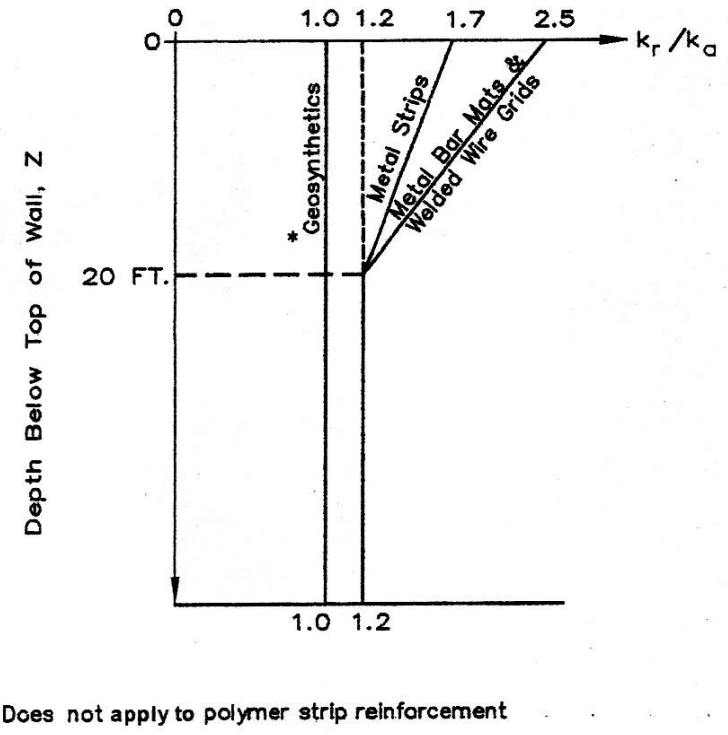

Figure 2.2 Active earth pressure multipliers for a given reinforcement versus depth (AASHTO, 2010)

k_a is found assuming Rankine conditions and uses equation 2.3 for a MSE wall with no face batter. A Rankine assumption negates friction of the face to the reinforced soil. This is a typical assumption in MSE wall design because there is effectively no friction generated between the soil and the face of the MSE wall even if concrete panels are used because of jointing (AASHTO, 2010).

$$k_a = tan^2(45 - \frac{\varphi}{2}) \tag{2.3}$$

where φ is the friction angle of the reinforced soil behind the face of the MSE wall.

The maximum tension per unit width of the wall, T_{max}, can then be found using Equation 2.4.

$$T_{max} = \sigma_H S_v \tag{2.4}$$

where σ_H is the factored horizontal stresses at the depth of reinforcement given previously by Equation 2.2, and S_v is the measured vertical spacing between reinforcement layers. The value T_{max} is used to calculate the connection at the wall facing and for pullout strength and rupture strength (AASHTO, 2010).

The location for the locus of maximum tension for inextensible reinforcements is given in Figure 2.3 and Figure 2.4 for extensible reinforcements.

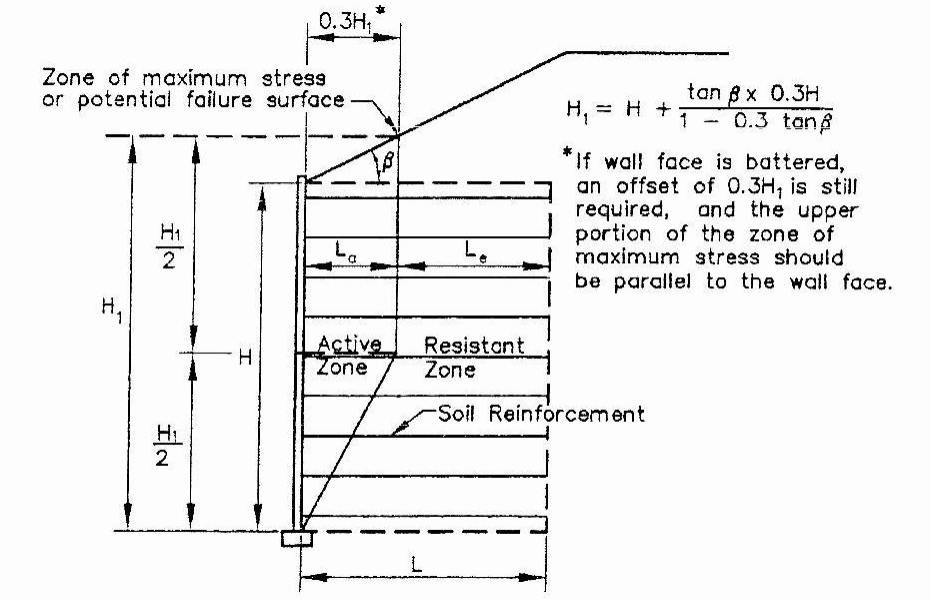

Figure 2.3 Location of locus of maximum tension for inextensible reinforcements (AASHTO, 2010)

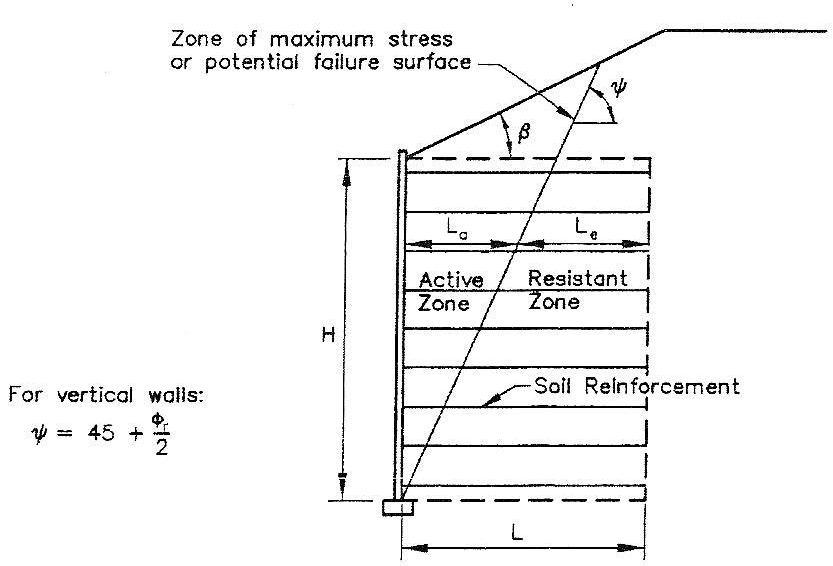

Figure 2.4 Location of locus of maximum tension for extensible reinforcements (AASHTO, 2010)

Reinforcement pullout resistance is checked at each depth of reinforcement and only the length beyond the active region is to be considered. The minimum length of embedment, L_e, beyond the active region is 3 feet and the total length, L, is equivalent to $L_a + L_e$ (AASHTO, 2010). The length of embedment can be calculated using Equation 2.5.

$$3 \leq L_e = \frac{T_{max}}{\Phi F^* \alpha \sigma_v C R_c} \tag{2.5}$$

where T_{max} is the maximum tensile force per unit width of wall as previously calculated in Equation 2.4, Φ is the resistance factor for pullout given in Table 2.2, F^* is the pullout friction factor, α is the scale effect correction factor, σ_v is the unfactored vertical stress seen in a given layer of reinforcement and calculated in Equation 2.1, C is the

reinforcement surface area geometry factor (2 for strip, grid, and sheet type reinforcements), and R_c is the reinforcement coverage ratio shown in Figure 2.6.

F^* and α are typically given from pullout testing done on the specific products, but can be estimated empirically as well. AASHTO also gives default values for both factors provided that the backfill meets standard AASHTO requirements. These default values are given in Table 2.3 and Figure 2.5

Table 2.3 Default values for α (AASHTO, 2010)

Reinforcement Type	Default Value for α
All Steel Reinforcements	1.0
Geogrids	0.8
Geotextiles	0.6

The value R_c is the ratio of the measured overall width of the grid reinforcement mat over the horizontal spacing between individual reinforcement mats. Figure 2.6 shows how the value R_c is measured for wire mats and Equation 2.6 gives the calculation.

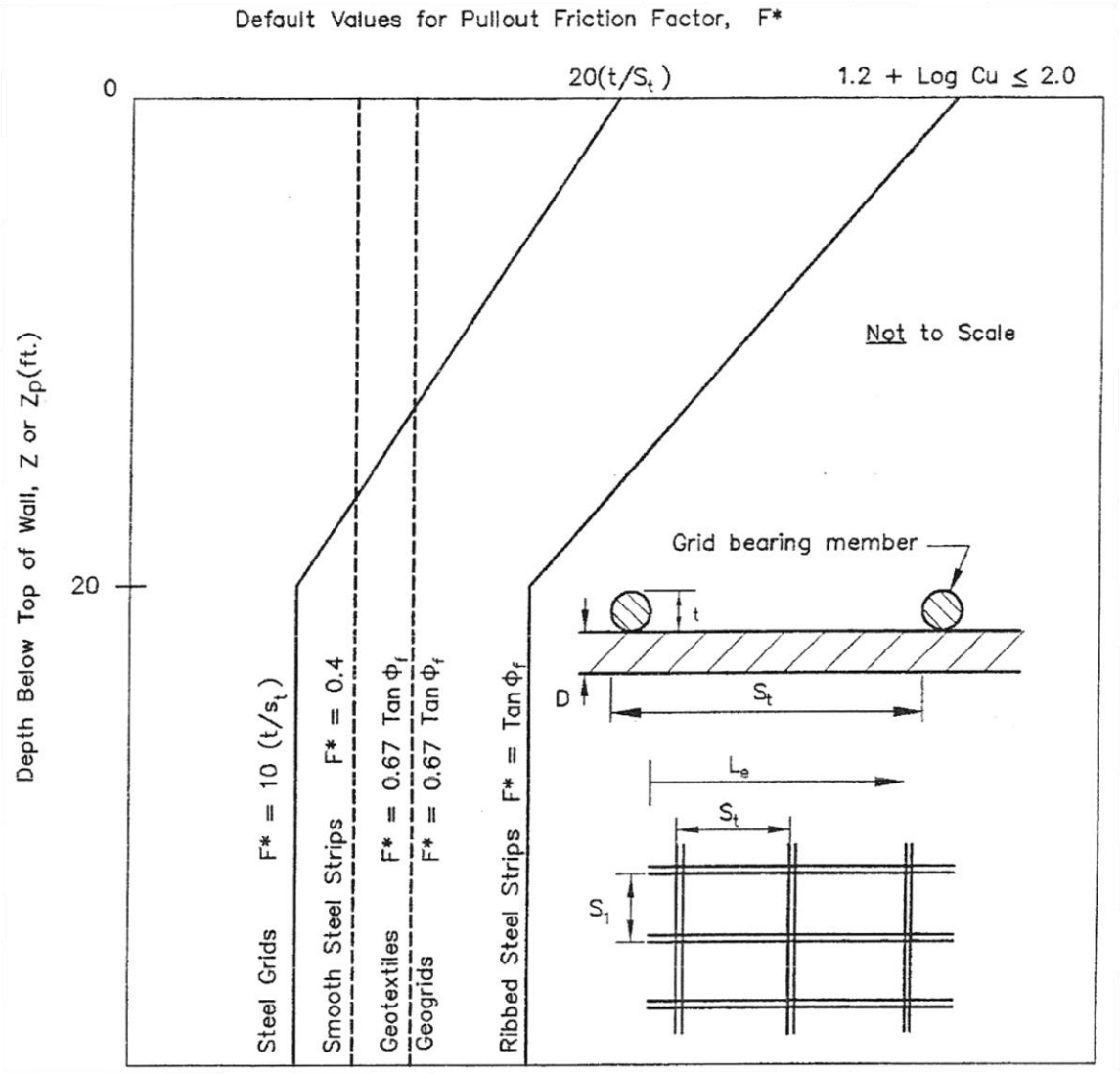

Figure 2.5 Default values for F* (AASHTO, 2010)

$$R_c = \frac{b}{S_h} \tag{2.6}$$

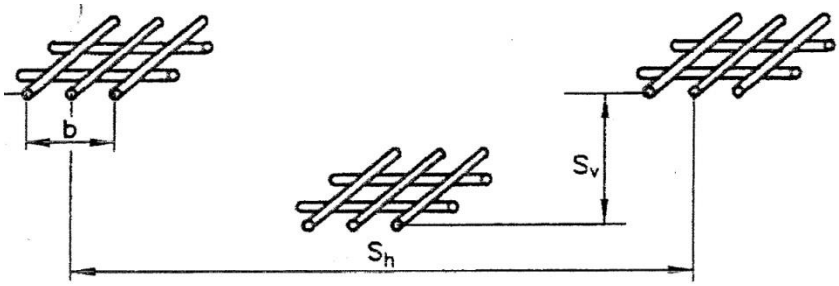

Figure 2.6 Measured distances for wire mat reinforcements for the value $\boldsymbol{R_c}$

The strength of the reinforcement is calculated using Equation 2.7. Equation 2.7 is a check to determine if the factored allowable tension in the reinforcement is greater than the factored tensions caused by the loads in the wall. If the check fails then the wall must be redesigned.

$$T_{max} \leq \Phi T_{al} R_c \tag{2.7}$$

where T_{max} is the factored maximum tension found at the locus of maximum tension for a given layer of reinforcement calculated in Equation 2.4, Φ is the resistance factor for the tension in reinforcement given in Table 2.2, T_{al} is the nominal long-term reinforcement design strength calculated using Equation 2.8, and R_c was given previously in Equation 2.6. T_{al} is multiplied by R_c to make a proper comparison between the two values as a force per unit width of wall (AASHTO, 2010).

$$T_{al} = \frac{A_c F_y}{b} \tag{2.8}$$

where A_c is the cross sectional area of the reinforcement corrected for corrosion over the design life of the wall, F_y is the minimum yield strength of the steel, and b is as defined for Equation 2.6.

The value A_c is calculated using standard corrosion rates developed by Yannas (1985) and supported by FHWA research studies. The corrosion rates given are dependent on backfill specifications that qualify the soil as "non-aggressive" and apply to steel types of reinforcements only (AASHTO, 2010). A_c is given in Equation 2.9.

$$A_c = \frac{E_c^2 \pi}{4} \tag{2.9}$$

where E_c is the diameter at the end of the service life of a wire or bar type reinforcement. Specifically E_c is calculated as shown in Figure 2.7 and Equation 2.10.

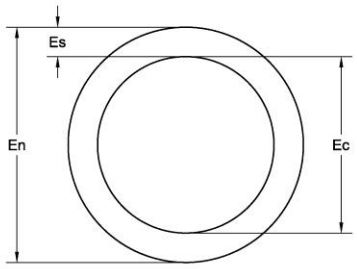

Figure 2.7 Geometry of how $\boldsymbol{E_c}$ is measured in a wire or bar reinforcement

$$E_c = E_n - 2E_s \tag{2.10}$$

where E_s is the cross sectional area lost due to corrosion, and E_n is the nominal wire cross sectional area (AASHTO, 2010).

Once the cross sectional area at the end of the service life (A_c) has been found, it is required to find the nominal cross-sectional area of the wire reinforcement that will be installed during construction, prior to corrosion. This can be found by using Equation 2.11.

$$A_n = \frac{E_n^2 \pi}{4} \tag{2.11}$$

The value for the sacrificial thickness of metal due to corrosion over the life time of the structure, E_s, is calculated using the standard rates of corrosion (AASHTO, 2010) for loss of galvanizing and for loss of steel which are as follows:

Loss of Galvanizing	=	0.58 mil./yr. for the first two years
	=	0.16 mil./yr. for subsequent years
Loss of carbon steel	=	0.47 mil./yr. after zinc depletion

Geosynthetic reinforcement deterioration rates are determined in the AASHTO specifications as well but are not addressed in this review.

As stated previously, the presented corrosion rates are for qualifying non-aggressive AASHTO backfill only. Non-aggressive backfill as specified by AASHTO requires that the pH of the fill be between 5 to 10, the resistivity must be greater than or equal to 3000 ohm-cm, the chloride content must be less than or equal to 100 ppm, the

sulfate content must be less than or equal to 200ppm, organic content in the fill must be less than or equal to 1% (AASHTO, 2010).

2.3 K-Stiffness Design Methodology

2.3.1 General

The K-Stiffness Method was developed by Allen and Bathurst for the Washington Department of Transportation in cooperation with the US Department of Transportation's Federal Highway Administration (Allen & Bathurst, 2003). The purpose of the paper was to provide a detailed study of the performance of MSE walls constructed either of extensible or inextensible reinforcements in controlled laboratory settings and in field applications. The study concluded that the AASHTO design methods used in practice overestimate the behavior actually seen in MSE walls, especially those constructed with extensible materials. The K-Stiffness method was presented in the paper as a possible design alternative that more accurately represents what is observed in MSE walls. This method achieves a more accurate approximation for the tension values seen in the internal design of a geosynthetic reinforced MSE wall and considers variables such as reinforcement type, sizing, spacing, and strength. External and global stability requirements are still required to meet the defined AASHTO requirements (Allen & Bathurst, 2003). The method was developed empirically from the behavior observed in the case studies analyzed in the paper. The K-Stiffness Method for geosynthetic walls will be presented in the following sections.

2.3.2 Internal Design

The general governing equation for the K-Stiffness method for internal design of geosynthetic walls is given in Equation 2.12.

$$T_{max}^{i} = S_v^i \sigma_h D_{tmax} \Phi \tag{2.12}$$

where T_{max}^{i} is the maximum load per unit width of wall in a given individual layer of reinforcement, i (Allen & Bathurst, 2003). This equation accounts for the typical internal design characteristics for a MSE wall such as the height of the wall, surcharge loads, vertical spacing, unit weights, etc., and is similar to the AASHTO specification defined in Equation 2.4 but includes two new factors, D_{tmax} and Φ. These factors modify the loads per unit wall width to more accurately reflect the behavior exhibited. D_{tmax} is a load distribution factor that changes the assumed geometry of the loads in the reinforcements as the depth increases. Φ is the general influence factor and incorporates the global stiffness factor, Φ_g, the local stiffness factor, Φ_{local}, the facing stiffness factor, Φ_{fs}, and the facing batter factor, Φ_{fb} as given in Equation 2.13. Equation 2.13 will be explained in greater detail later in this chapter (Allen & Bathurst, 2003).

$$\Phi = \Phi_g \, \Phi_{local} \Phi_{fs} \Phi_{fb} \tag{2.13}$$

σ_h, given in Equation 2.12, is the average load over the height of the wall per unit width of wall and is calculated using Equation 2.14. Rather than calculating the lateral earth pressure per layer of reinforcement material, it is simply averaged over the height of the wall.

$$\sigma_h = 0.5K\gamma(H + S) \quad (2.14)$$

where S is the equivalent height of the uniform surcharge pressure and is therefore equal to q/γ, H is the height of the wall, γ is the unit weight of the wall, and K is the lateral earth pressure coefficient. The lateral earth pressure coefficient is calculated using Equation 2.15.

$$K = K_o = 1 - sin\varphi_{ps} \quad (2.15)$$

where φ_{ps} is the peak plane strain friction angle. It is to be noted that Allen and Bathurst use the lateral earth pressure coefficient, K, taken as the at-rest soil conditions, K_o (Allen & Bathurst, 2003). They also state that it is not implied that at-rest conditions exist, but it is used as a reference point to characterize the soil behavior.

A comparison between the at-rest lateral earth pressure coefficient, K_o and the active lateral earth pressure coefficient, K_a as the index parameter to calculate T_{max}^i was done by Allen and Bathurst to evaluate the influence of the factors in the behavior of the wall. The comparison shows K_o provided a more simple way of evaluating the soil strength parameters that influence the wall than K_a. K_o does a better job of approximating the true soil strength parameter, the bulk soil modulus, and is also independent of the face batter. It is assumed that K_a is less suitable because the face batter and the soil-facing interface may have more variables but have not yet been conclusively found. It was noted that even though K_o does better at approximating the soil strength parameters, there is still variance that may be due to other influences such as compactive efforts (Allen & Bathurst, 2003).

2.3.3 Influence Factor, Φ

The influence factor, Φ as previously given in Equation 2.13 incorporates four variables that account for the relative stiffness of the reinforcement. Φ_g is the global stiffness of the reinforcement, Φ_{local} accounts for the local variations of stiffness in the reinforcement, Φ_{fs} is the stiffness of the facing elements, and Φ_{fb} is the batter of the face of the wall (Allen & Bathurst, 2003). These are all empirically derived influence factors that have some degree of bias on the maximum tensile forces exhibited in the reinforcement of a MSE wall.

The global stiffness factor Φ_g is calculated as the global stiffness of the reinforcement, S_{global}, divided by atmospheric pressure as shown in Equation 2.16. This is done to create the dimensionless factor.

$$\Phi_g = \alpha \left(\frac{S_{global}}{P_a} \right)^{\beta} \tag{2.16}$$

where α and β are constant coefficients, both equal to 0.25 and S_{global} is found as shown in Equation 2.17.

$$S_{global} = \frac{J_{ave}}{(H/n)} = \frac{\sum_{i=1}^{n} J_i}{H} \tag{2.17}$$

where J_{ave} is the average tensile stiffness, J_i is the individual stiffness of the reinforcement layers, and H is the height of the wall (Allen & Bathurst, 2003).

This method of calculation is the straight forward way to obtain these values if the material properties in the reinforcement are established and are not considered as a composite material. The crimped wire reinforcement makes it difficult to acquire the average stiffness value J_{ave} by this straight forward calculation because this is the first project to implement its use and has no previous stiffness testing performed. The K-Stiffness method provides empirical data collected from the numerous case studies as shown in Figure 2.8 that can be used to back-calculate the global stiffness factor from the measured maximum tension in the wall using Equation 2.18.

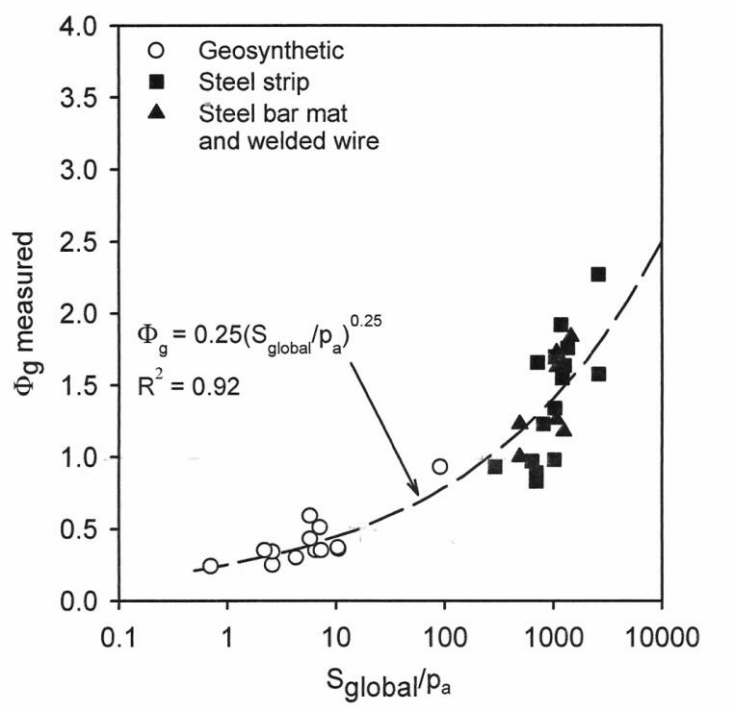

Figure 2.8 Measured global stiffness factor, $\boldsymbol{\Phi_g}$ versus the normalized global stiffness (Allen & Bathurst, 2003)

$$\Phi_g(measured) = \frac{T_{mxmx}}{S_v^i \sigma_h D_{tmax} \Phi_{local} \Phi_{fs} \Phi_{fb}} \tag{2.18}$$

where T_{mxmx} is the maximum tension found in the wall and D_{tmax}, Φ_{local}, Φ_{fs}, and Φ_{fb} are all taken as 1 for a steel, vertical, wire-facing wall (Allen & Bathurst, 2003). These values will be examined in greater detail in the next few paragraphs. By back-calculating Φ_g, the value for the normalized global stiffness S_{global}/P_a can be read from Figure 2.8.

A distinction needs to be made to clarify the difference between the values T_{max}^{i} and T_{mxmx}. As stated previously, T_{max}^{i} is the maximum tensile load per unit width of wall for a specific layer of reinforcement. T_{mxmx} is the maximum value of the T_{max}^{i} values throughout the wall.

The local stiffness factor, Φ_{local} is a factor that accounts for the variability of stiffness in an individual layer of reinforcement (S_{local}) relative to the global stiffness throughout the wall (S_{global}) and is presented in Equation 2.19.

$$\Phi_{local} = \left(\frac{S_{local}}{S_{global}}\right)^{a} \tag{2.19}$$

where the coefficient a is equal to 1 for geosynthetic reinforced walls and 0 for steel reinforced walls (Allen & Bathurst, 2003). Allen and Bathurst make mention in chapter 8.4.4 of their study that steel reinforcements that have low values of global stiffness may possibly require a coefficient somewhere in between the values of 0 and 1, but would require further data and testing to be conclusive. For the crimped wire mat reinforcements presented in this project, it is assumed that the compliance of the crimps relative to the stiffness of the steel governs the local stiffness values and could be

considered as a fully extensible product similar to a geosynthetic. For this reason, the coefficient a is taken as 1.

The purpose is to capture any redistribution of load from one layer of reinforcement to another that could be dependent on the reinforcement type, sizing, spacing, and compactive efforts for a given layer. A straight forward approach for calculating S_{local} is provided as shown in Equation 2.20.

$$S_{local} = \left(\frac{J}{S_v}\right)_i \tag{2.20}$$

The same issue is present with S_{local} as with the global stiffness factor; this is the first time that the crimped wire mats have been implemented in a full scale wall and no data for stiffness values have been evaluated. It is therefore requisite to back-calculate the stiffness values using the empirical data Allen and Bathurst presented in the K-Stiffness method using the measured maximum tensile load in the wall as shown in Equation 2.21 and then correlate with Figure 2.9.

Φ_{fs} is the facing stiffness factor and accounts for the loads transmitted to the facing mechanisms implemented in a MSE wall system (Allen & Bathurst, 2003). Allen and Bathurst found that more load is transferred to the facing elements as the global stiffness of the reinforcement decreases. For example, an inextensible steel reinforced wall has a high global stiffness value relative to the stiffness of the facing; therefore the facing elements contribute little to the design and does not need to be considered.

If an extensible product is used to reinforce the wall, the stiffness of the facing elements will contribute to the overall design of the MSE wall and need to be considered.

For this reason, Allen and Bathurst suggests that Φ_{fs} should be equal to 1 for all inextensible steel reinforced walls (Allen & Bathurst, 2003).

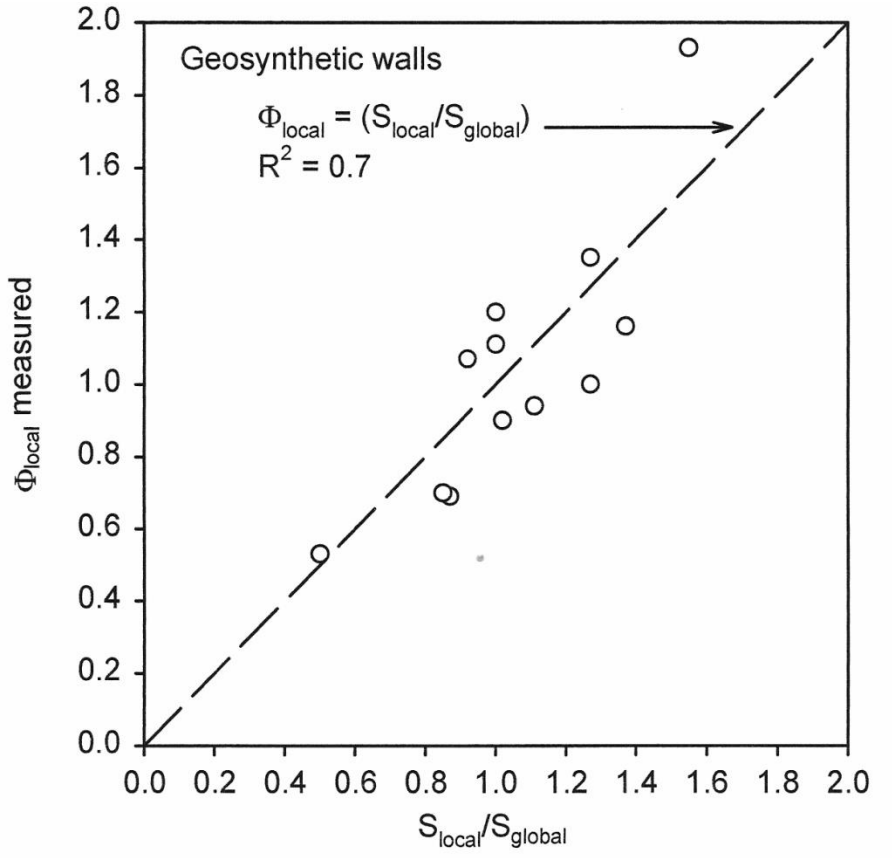

Figure 2.9 Measured local stiffness factor versus the value $\boldsymbol{S_{local}/S_{global}}$ (Allen & Bathurst, 2003)

$$\Phi_{local}(measured) = \frac{T_{mxmx}}{S_v^i \sigma_h D_{tmax} \Phi_g \Phi_{fs} \Phi_{fb}} \tag{2.21}$$

For extensible reinforcement products, the stiffness of the facing elements will attract more load depending on the type of facing used. By comparison, a welded wire face or a wrapped face is less stiff than a modular block face or a fully propped concrete

panel (Allen & Bathurst, 2003). It was concluded that the facing stiffness factor for an extensible reinforced wall can be categorized into three values:

Φ_{fs} = 0.35 for modular block and propped concrete panel-faced walls (stiff facings)

= 0.5 for incremental precast concrete facings

= 1.0 for all other types of wall facings (flexible facings – e.g., wrapped-face, welded wire or gabion faced walls)

Φ_{fb} is the factor that accounts for the face batter of the wall, or how the face of the wall is sloped. A negative face batter represents a wall facing that overhangs and a positive face batter slopes away from the toe of the wall. Typically face batter is accounted by Coulomb earth pressure theory, but the current limit equilibrium methods fail to accurately predict the loads in the reinforcement such that the predicted loads are much less than actually seen (Allen & Bathurst, 2003). Allen and Bathurst applies the same methods used for the previous factors to represent the face batter influence in the behavior of the wall. Equation 2.22 is used to describe the influence from batter of the face.

$$\varphi_{fb} = \left(\frac{K_{abh}}{K_{avh}}\right)^{d} \tag{2.22}$$

where K_{abh} is the horizontal component of the active earth pressure coefficient accounting for the face batter of the wall, K_{avh} is the horizontal component of the active earth pressure coefficient, and d is a constant coefficient. Equation 2.22 assumes that the wall is vertical and that as the wall approaches vertical, φ_{fb} goes to 1. The value d was

found to be 0.25 using a regression analysis. It is mentioned by Allen and Bathurst the correlation value was considered low due to the lack of data for walls with a significant face batter. Until more data is available for significantly battered walls, it is recommended that the coefficient d remains at 0.25 as it provides the best fit when compared with other values against the strain behavior seen in the wall (Allen & Bathurst, 2003). The face batter of the wall for this project is to be considered vertical and therefore φ_{fb} is equal to 1.

2.3.4 Influence Factor, D_{tmax}

D_{tmax} is the distribution factor that accounts for the variation of the tensile loads seen in the wall as the height of the wall changes. Typical AASHTO design theorizes that the tensile loads increase linearly with depth according to the unit weight of the soil. This results in a triangular pressure distribution behind the face of the wall with the maximum at the bottom of the wall. Allen and Bathurst assume a trapezoidal load distribution similar to what is exhibited in braced excavations as mentioned previously. For extensible reinforcement products the maximum load in the wall is seen between a wall height of 0.4H and 0.8H below the top of the wall where H is the total height of the wall as shown in Figure 2.10.

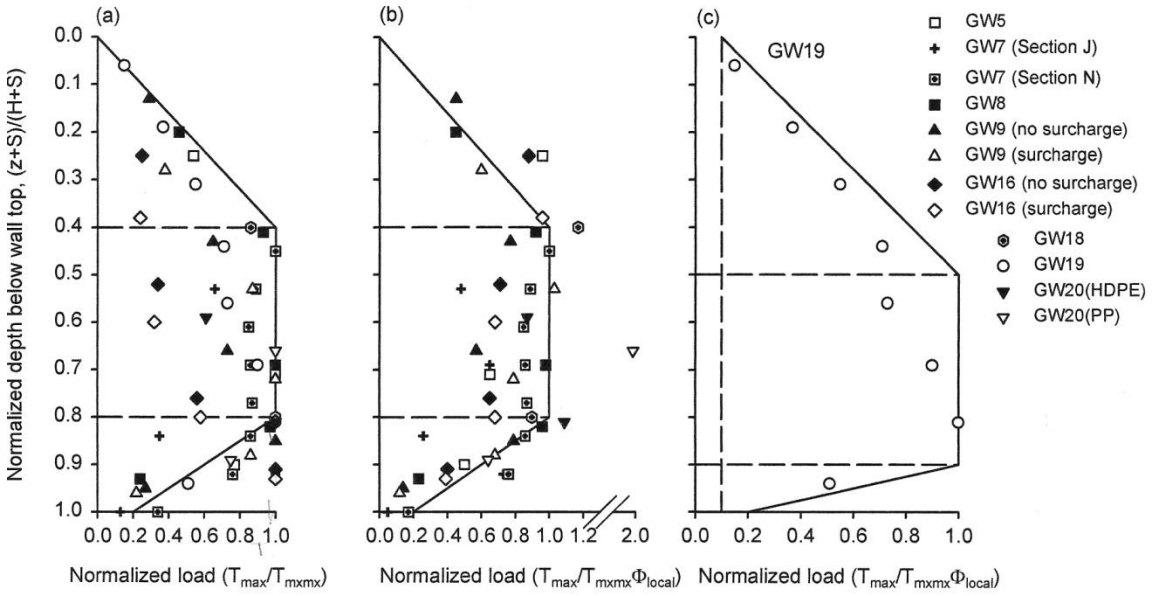

Figure 2.10 Trapezoidal distributions of distribution factor $\boldsymbol{D_{tmax}}$ (Allen & Bathurst, 2003)

In Figure 2.10a the maximum tensile load, T_{max}^{i} is normalized with respect to T_{mxmx}. It can be seen that some scatter still remains. Allen and Bathurst then normalized T_{max}^{i} with respect to T_{mxmx} and Φ_{local} as shown in Figure 2.10b. The scatter around the distribution diagram is lessened by accounting for the effects of Φ_{local}. Figure 2.10c shows how the stiffness of the reinforcement affects the load distribution of the wall. Figure 2.10c was a unique case that utilized stiff polymer strap reinforcement. It is shown by Allen and Bathurst that as the stiffness of the reinforcement increases, the distribution of the load tends to become more linear as traditional methods theorize (Allen & Bathurst, 2003). The crimped metal wire mat reinforcement presented in this paper is assumed to be a flexible extensible reinforcement and is expected to demonstrate a trapezoidal distribution as shown in Figure 2.10b.

CHAPTER 3

WALL INSTRUMENTATION AND CONSTRUCTION

3.1 Introduction

Instrumentation was placed in the wall to provide quantitative feedback of reinforcement tensions and wall deformations during and after the construction of the wall. Three separate methods were used to collect specific data that would quantify the behavior of the wall. The first method used was custom built, in-line load sensors to record the tensile forces in the reinforcement; the second method used surveying equipment to measure deflections of the wall face; and the third method was to take initial and final physical measurements of the crimp deformations in each wire mat. Other measurements such as sand cone density tests and surveyed elevation measurements were performed as the wall was built to assure proper construction and to determine values for data analysis.

3.2 Instrumentation

3.2.1 Concept and Design

One of the goals of the project was to accurately record the tensile forces and to locate the locus of maximum tension in a 20 foot high wall reinforced with the prototype crimped wire mats. The small diameter of the wires in a mat presented a challenge to achieve this goal due to the difficulty of placing a single strain gauge on the wire. It was decided to fabricate 48 custom built, in-line, load sensors to meet the requirements of this project. The number of sensors was limited by the amount of time and labor required to

construct each sensor; however, the 48 sensors proved to be sufficient for the needs of the project.

4.2.2 Sensor Preparation and Strain Gauge Application

The in-line load sensors were constructed from cold drawn G60 1/2" x 3/4" bar stock steel and shaped in the traditional "dog bone" style to avoid end stress effects. The overall length of the sensor is 4" long. The thickness at the narrowest point in the load sensor was machined down to 1/4" and extended for 1 1/4" from end of radii to end of radii. Holes were drilled in each end of the sensor to match the W3.5 and W5.0 wire diameters that were used in the reinforcement. These holes were also designed to assure adequate clear spacing distances and development length.

Two holes were drilled and tapped through the side on each end to allow 5/16"-24 hex head bolts and set screws to clamp the reinforcement wires in the sensor. This method of anchoring the longitudinal wires in the sensors was tested in a tensile strength testing machine to assure no possible slipping or pullout of the wires. The wire reached its rupture capacity with no recorded movement between the wire and the anchor mechanism and was therefore considered successful.

One 1/8" hole was drilled and tapped through on the top of one end of the sensor to allow a nylon wire clamp to provide stress relief for the instrumentation cables. Figure 3.1 shows the design drawings for the load sensor.

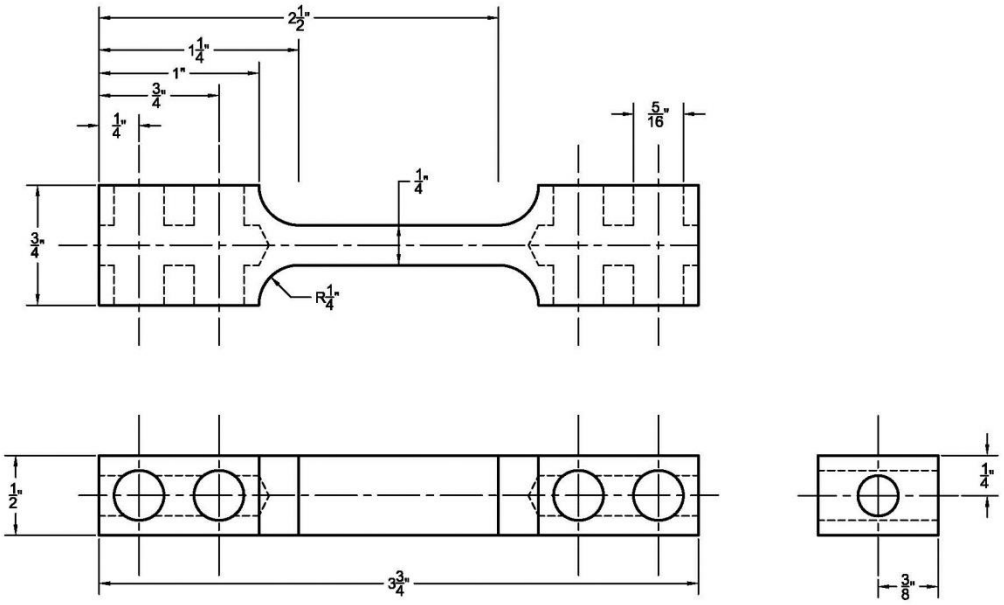

Figure 3.1 Custom Built, In-Line, Load Sensor Design

After the load sensors were machined according to the design shown, strain gauges were placed exactly in the center on both sides of the narrow portion of the bare sensor. It was required that the sensors be finished and chemically prepped before placement of the strain gauges.

The finishing process involved removing the burrs and all sharp edges to prevent possible severance of the instrumentation cables and to allow safe handling of the sensors. The bare sensors were then degreased using CSM degreaser and sanded using two varying coarseness of sand paper. The faces the strain gauges were placed on were wetted with M-prep Conditioner A and then sanded by hand using 60-grit sandpaper. The facings were then wiped clean with sterile gauze in a single direct motion. The facings were wetted again with the conditioner and sanded by hand again with a finer

220-grit silicon-carbide paper. The alignment markings were then burnished on to the faces. The load sensor faces were then wetted with the conditioner solution again and scrubbed with a cotton applicator until the residue was removed. The remaining conditioner was wiped from the facings with sterile gauze. The facings were then scrubbed liberally with M-Prep Neutralizer 5A with the cotton-tipped applicator and wiped clean in a single direction with sterile gauze. These steps were necessary to correctly prepare the bare sensor for strain gauge application.

The strain gauges used for the sensors were Vishay Micro-Measurements combined poisson/axial gauges with a 350 Ohm resistance. The strain gauges were to be placed in a fashion to complete a full Wheatstone Bridge. Figure 3.2 shows the general electrical schematic for a full Wheatstone Bridge.

The full Wheatstone Bridge is used to compensate for any bending stresses during loading and to compensate for temperature fluctuations throughout the experimental time period. It also doubles the value of strains produced due to forces applied and thus allows for more accurate readings. The full Wheatstone configuration requires that two strain gauges be placed on each facing exactly mirrored of each other.

The strain gauges were placed on the prepped bare sensors by setting a single strain gauge on a chemically cleaned glass square, then picked up by using a strip of Micro-Measurements PCT-2M gauge installation tape that was just long enough to be easily maneuvered by hand. Using a stationary magnifying glass, the gauge was carefully placed by lining up the alignment markings on the strain gauge to the burnished alignment markings made during the prep phase.

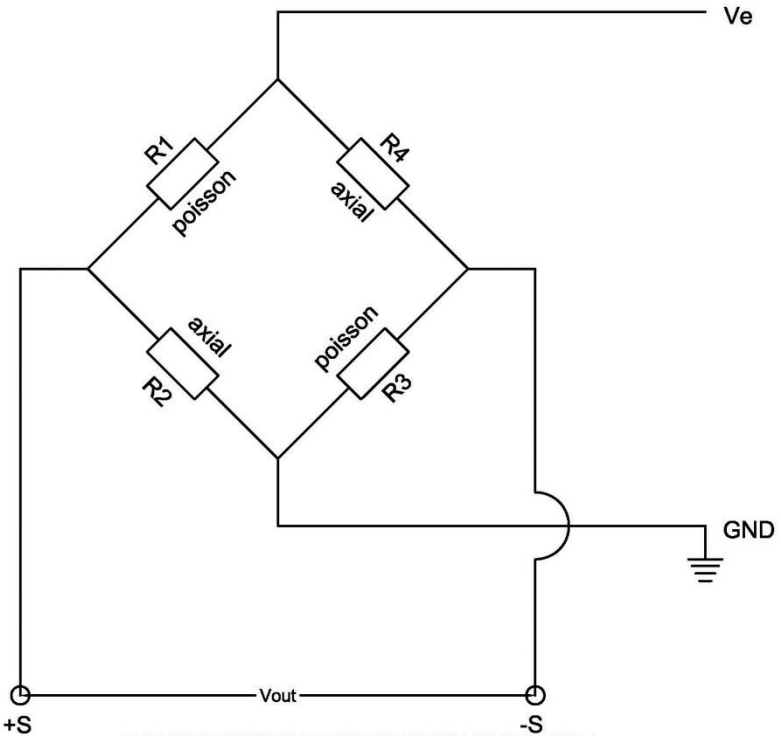

Figure 3.2 General Electrical Schematic for a Full Wheatstone Bridge

Once the strain gauge was properly placed, the tape was peeled back from one end at a shallow angle with the gauge following with it. The tape was folded back to permit the application of the M-Bond 200 catalyst. A thin sheen of catalyst was applied and allowed to dry for one minute. One to two drops of M-Bond 200 adhesive was then placed on the spot where the gauge would be. The tape was quickly replaced over the burnished markings at a shallow angle with one hand while using sterile gauze in the other hand to firmly and accurately seat the gauge to the facing. Thumb pressure was then applied for a minimum of one minute to allow the adhesive to dry. This method expels any excess adhesive and assures correct placement.

All products used for these sensors were Vishay Micro-Measurements products and therefore met the requirements for the Vishay Micro-Measurements strain gauge application.

While prepping the sensors and placing the strain gauges, care was taken to eliminate any possible sources for contamination. Sterile nitrile gloves were worn during the process and were changed after each strain gauge was placed. One facing of all 48 sensors was completed before strain gauges were placed on the opposite facing. The tape was not removed after drying to reduce contamination from the chemical prepping procedure from the opposite facing. Once both sides of all sensors were completed and allowed to dry over night, the tape was taken off and any excess dry adhesive was removed. This was the final step before soldering the instrumentation cables to the strain gauges.

3.2.3 Soldering

Soldering of the instrumentation cables was done after all strain gauges were placed on the sensors. All strain gauges required tinning of the terminals as well as the ends of the instrumentation cables before soldering could proceed. The instrumentation cables were stripped of their insulation and shielding with enough of the twisted four strand cable exposed to easily maneuver: 1/4” to 3/8” of the individual wires were stripped of their insulation and then tinned.

After attempting to solder the first few sensors, it was found difficult to manipulate the individual wires in a fashion that did not cause excessive stress on the terminal pads of the strain gauges. For this reason it was required to place an additional

terminal strip on the top of the narrow portion of the sensor to facilitate the soldering process. The wires from the instrumentation cables were soldered to the terminal strip and then smaller, more pliable wires were used as jumpers from the terminal strip to the terminals on the strain gauges. Figures 3.3 and 3.4 show portions of the soldering process.

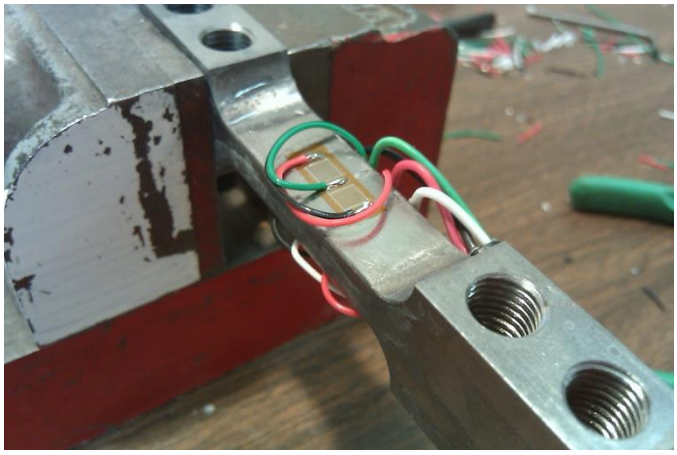

Figure 3.3 Soldering of the In-Line Load Sensors

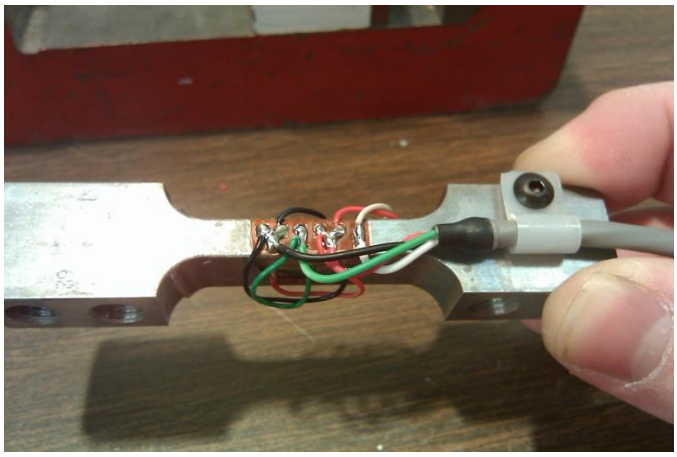

Figure 3.4 Soldering complete on an In-Line Load Sensor

3.2.4 Calibration

Calibration of the sensors took place after soldering was completed on all sensors and before any weatherproofing was performed. The calibration process was completed using custom brackets that would fit a GeoJac© incremental direct shear device and allow the sensors to bolt to these brackets. This allowed the sensors to be calibrated relative to a high grade load cell. Before any load was applied to the sensor, bending loading and temperature compensation was tested by applying a bending force by hand and a heat gun was used to apply a temperature fluctuation. All sensors were found competent against bending and temperature influences.

The sensors were loaded incrementally starting at 0 lbs of load to the highest of 900 lbs and then unloaded in larger increments back to 0 lbs. The data was recorded in an Excel spreadsheet and the linear estimate function was used to get the statistical results such as the slope, linear regression, and zero intercepts. The calibration number was obtained by dividing the excitation voltage in millivolts by the slope of the load versus voltage curve. This produced the calibration number for each sensor in pounds per volt per volt excitation ($lb/V/V_e$). A linear regression was fit to the slope to approximate the accuracy and resolution of the calibrations performed. All sensors performed very well and within the predetermined tolerance of plus or minus 10 lbs. The average R^2 factor for all sensors indicate accuracy to four significant figures.

3.2.5 Weatherproofing

After all sensors were calibrated, the sensors were weatherproofed using wax and M-Coat J©. Paraffin wax was brushed on the sensors enough to completely cover the

strain gauges and any exposed wire outside of the external insulation of the instrumentation cable. The same was done with the M-Coat J product with extra care that no pockets or holes were open to external influences. After the weatherproofing was allowed to cure, the sensors were set through the calibration process again to confirm the previous calibration numbers and to verify no defects were caused during the weatherproofing process. Some variation occurred after weatherproofing; therefore, it was decided to use the post-weatherproofing calibration numbers.

3.2.6 Sensor Installation

The in-line load sensors were placed in the crimped mats after all calibration and weatherproofing was finished. Each sensor was previously stamped with an identification number 1 through 48. These identification numbers corresponded to their respective location in the wall by elevation and wire position. The sensors were spaced throughout the wall to sufficiently capture the locus of maximum tension as the wall was built and as a completed structure. Figure 3.5 shows the mapped locations of the sensors throughout the wall.

The sensors were installed in the mats by removing a 1 3/4” length of longitudinal wire 4” behind the front of the transverse wire. The length of wire removed was equal to the distance between seating points in the sensor. An 8” length of 2” diameter PVC pipe was then slid over the longitudinal wire and moved toward the next transverse wire to keep it out of the way of installation. Approximately 8” of instrumentation cable was curled up and secured to the sensor with a rubber band to provide slack during wall deformation. The in-line load sensor then substituted the section of removed longitudinal

wire. The sensor was seated and then anchored into position on both of its ends by using the set screws and hex head bolts previously discussed. The set screws were inserted first and tightened using an allen wrench. The hex head bolts were then inserted and torqued to their respective capacities of 25 ft-lbs using a torque wrench. Figure 3.6 shows the load sensor after installation.

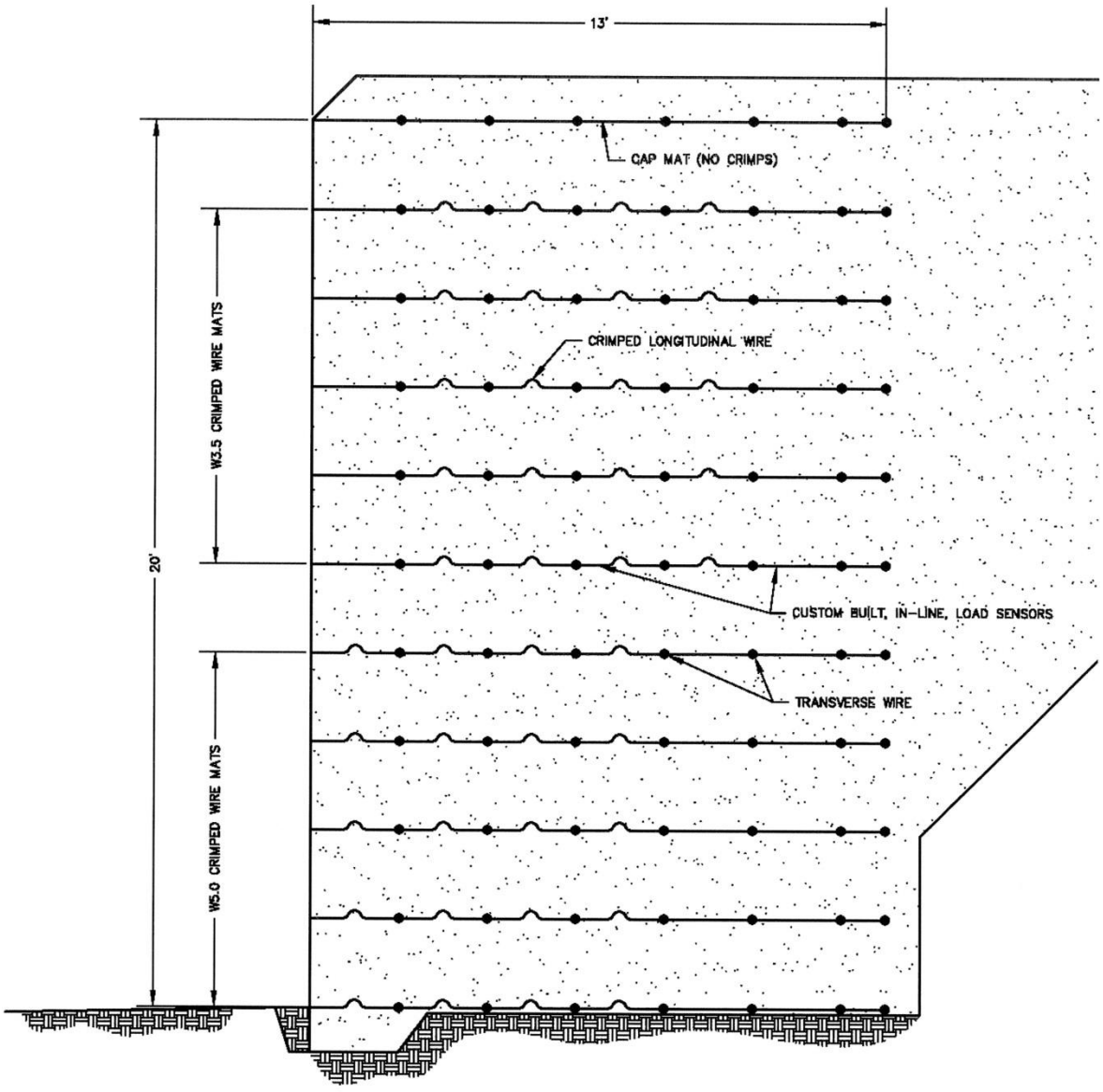

Figure 3.5 Proposed Wall Design

Figure 3.6 Installed In-Line Load Sensor

The PVC pipe was then slid back into place, covering the sensor. The purpose of the PVC pipe was to provide protection to the sensor during the construction of the wall.

3.3 Wall Construction

3.3.1 Site Location

The construction site was chosen to be placed on Utah State University (USU) campus. The original desired location was to be in a construction company's gravel pit, but due to MSHA restrictions, the location needed to be moved. The USU location chosen was in the hillside of an abandoned gravel pit on the corner of 1400 North and 1200 East in Logan, Utah. Initial site inspections showed the native soil to be satisfactory for the construction of the wall. The hillside of the site was observed to be

silty-sand with a high portion of cobbles according to hand texture tests and ASTM D2488. Due to time and budget constraints, no subsurface explorations were done prior to construction.

Volume calculations were done by taking an initial survey of the site using GPS survey equipment and then importing the data into AutoDesk Civil3D. It was found that if the slope of the hillside was cut back enough to accommodate the length of the reinforcement mats, there would be enough native fill to construct the 20' wall. The limits of excavation drawn in Civil3D were then exported back into the GPS equipment as coordinates and then staked-out on the site.

3.3.2 Construction

The construction of the wall began by excavating the portion of the slope that had been previously staked out. An engineer's level was set up and referenced to a site benchmark to monitor the elevation of the excavation and wall construction. The excavation ended when zero elevation was met and the construction of the wall could then proceed.

A one-foot deep footer was excavated at the toe to establish the foundation for the wall and to provide a starting point for the interlocking wire face mats. The footer was not an instrumented portion of the wall. The instrumented portion of the wall included the full elevation of the center three wire mats with a single wire mat on either side of the instrumented portion for the full elevation. The additional mats on either side of the instrumented portion were included in the wall design to reduce boundary effects in the data. Each crimped reinforcement mat was 48" wide having 16" between each of the

four longitudinal wires. Individual mats were spaced 16" apart. Wing walls were placed outside of the center five crimped mats. The wing walls were not crimped and therefore were considered a rigid and inextensible boundary condition.

The base level instrumented wire mats were placed after compaction of the footer and foundation was complete. The method used to anchor the crimped reinforcement mats to the facing required placing the front transverse wire of the crimped reinforcement mats over the top prongs of the previous lift's face mats. The current lift's face mats were then interlocked into the previous lift's face mats. As the current lift was filled and compacted, the facings would deflect out to meet the front transverse wire of the crimped reinforcement mat. The front transverse wire would then be the mechanism that pinned the face of the wall into position.

Before each lift was compacted, it was necessary to connect the instrumentation cable leads to the data recording system. The data recording system consisted of three 16-channel multiplexers connected to a Campbell Scientific 21X datalogger. To reduce shifting of the mats while connecting the cables, piles of fill were placed on the rear of the mats. Zero readings for the in-line load sensors were taken and the initial deflections of the face were surveyed after the connections of the current lift were finished. Readings were continually collected as each lift was added. Readings continued after construction for three months.

Each lift was filled and compacted after zero readings of the sensors were collected and face deflections were surveyed. As each lift was filled, five gallon bulk samples were collected for grain size analysis and strength testing. Each two foot lift was separated into one foot lifts and was compacted using a 41.5 kip front end loader. The

compaction of the lifts required three passes with the front end loader. One sand cone test was done on the first one foot lift and two sand cone tests were done on the second one foot lift. Elevation measurements of the finished lift were taken with the engineer's level and the next layer of crimped reinforcement mats were placed.

Since this was the first time crimped wire mats were used in a full scale study, the amount of face deflection due to compaction was unknown. For this reason, the front transverse wire was initially set two inches behind vertical to account for potentially excessive deformation in the face of the wall. As the construction of the wall progressed, it was found that the two inch batter was too conservative and the wall began to slightly batter back. This was changed to one inch midway through the construction of the wall until it was finished.

A one foot soil cap was placed on the top once the wall reached its full height. This cap wasn't compacted with the front end loader as the previous lifts were, but was simply graded by the hoe end of an excavator. The rest of the site was graded in a way to allow proper drainage away from the wall. It was recognized that the wall may pose a risk to local college students' winter activities so a chain-link fence was placed at the top of the wall for safety. All vertical drops greater than 30 inches as a result from construction of the wall were fenced accordingly.

CHAPTER 4

RESULTS

4.1 Soil Characteristics

The soil samples collected during construction were taken back to the soils testing laboratory at Utah State University and were weighed and classified. Lifts one, five, and ten were chosen to be representative samples to obtain a soil gradation and a soil classification. All sand cone samples were weighed and measured to obtain soil densities and percent water content for each lift.

Grain size analyses were performed on lifts 1, 5, and 10 according to ASTM D2488. The soil was allowed to thoroughly air dry. Due to a high silt content and aggregation of fines, the soil was washed through the #40, #100, and #200 sieves. Figure 4.1 shows the gradation of the three lifts. According to the Unified Classification system (ASTM D2488) this soil is a GM soil. Specifically, this is a sandy soil with a high content of non-plastic fines with a large portion of poorly graded gravels up to 4".

The initial weight of the sand cone samples were measured at the time of collection at the construction site. This was done to obtain accurate water content results. After completion of the wall, the samples were taken back to the lab and oven dried over a period of three days. The dry weights of the soil were then measured and the water content was calculated as was the dry unit weights. The total unit weights for each lift could then be calculated by incorporating the water content into the dry unit weights. The unit weights for each lift were heavy due to the amount of sandstone cobbles in the samples so corrections were done on the densities to compensate for this. The final unit

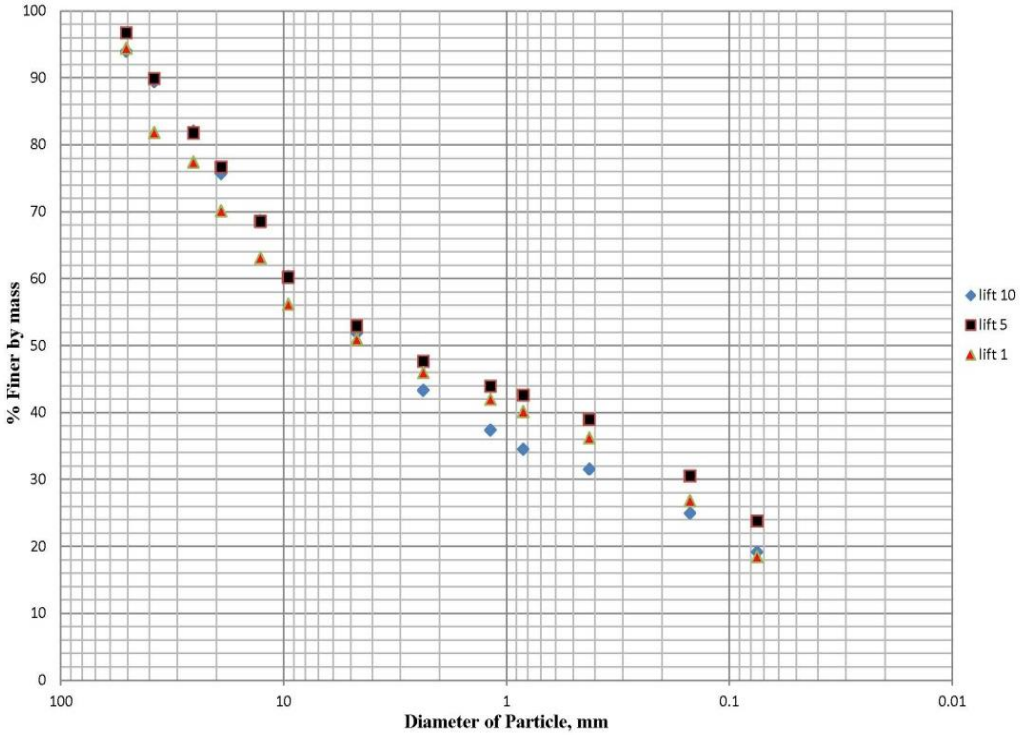

Figure 4.1 Grain size distribution of lifts 1, 5, and 10

weights showed a wide variance between the ten lifts. For this reason an average unit weight was taken by excluding the two highest and two lowest unit weights and then averaging the rest. Through these means a unit weight of 143.7 pcf was obtained. Again, it was realized that this unit weight still did not seem logical given the data. Relative density tests were performed on the bulk density samples to verify the maximum and minimum densities of the soil. The relative density tests showed that the unit weight of 143.7 pcf was too high, but rather a dry unit weight of 118 pcf was more logical. This corresponded to 75% relative density which would be roughly 95% compaction relative

to a modified proctor test. The unit weight of 118 pcf gave a total unit weight of 123 pcf by considering the water content.

4.2 Elevation Readings

The vertical spacing between lifts were required to calculate the K values as the wall progressed and this was done by collecting the elevation measurements after each lift was compacted. Six points on each lift were surveyed and then averaged. The average elevation of each mat was used to calculate the vertical spacing between mats. The vertical spacing was taken as half of the distance between the previous lift and the current lift elevations plus half the distance between the current lift and the next lift. For the bottom lift, the vertical spacing was calculated assuming a nominal 2’ sub-grade elevation spacing. Table 4.1 shows the elevations from each lift and the vertical spacing between each lift.

Table 4.1 Elevation of lifts and vertical spacing between lifts

Lift	Average Elevation, ft	Average Thickness, ft	Sv, ft
final	20.932	1.307	
10	19.626	1.888	1.597
9	17.738	0.949	1.418
8	16.789	1.453	1.201
7	15.336	3.139	2.296
6	12.197	2.020	2.579
5	10.177	2.000	2.010
4	8.177	1.500	1.750
3	6.677	2.235	1.868
2	4.442	1.810	2.023
1	2.632	2.639	2.225
0	0.000	2.000	2.320

4.3 Tension Readings

Tension readings were collected throughout the construction of the wall and after construction. The purpose of recording tension values as the wall was built was to confirm the wall was behaving as expected relative to its elevation and that no excessive loads were being developed for safety considerations. Figures 4.2 through 4.11 show the tensile forces versus the location of the force by depth behind the face of the wall. It

should be noted that the forces recorded are assumed to be continuous between transverse wires because it is assumed the pullout resistance is developed around the transverse wires only. The transverse wires are shown in two foot increments according to their spacing in the mats.

Each plot represents an individual layer of reinforcement. The plots show the forces as each lift of overburden is added. The red line marks the forces once the wall reached its finished height. After three months of observation it was found that the peak forces occurred only one week after the finished construction of the wall. For this reason, the forces after the peak recorded force have been omitted.

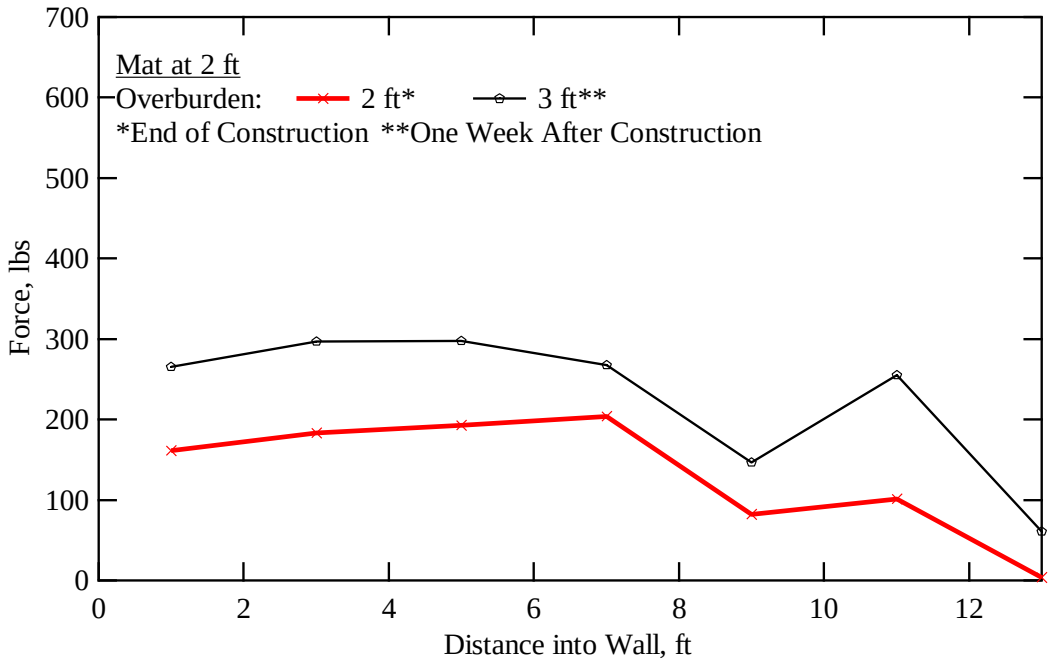

Figure 4.2 Tensile forces in crimped reinforcement mat 2 ft above base of the wall

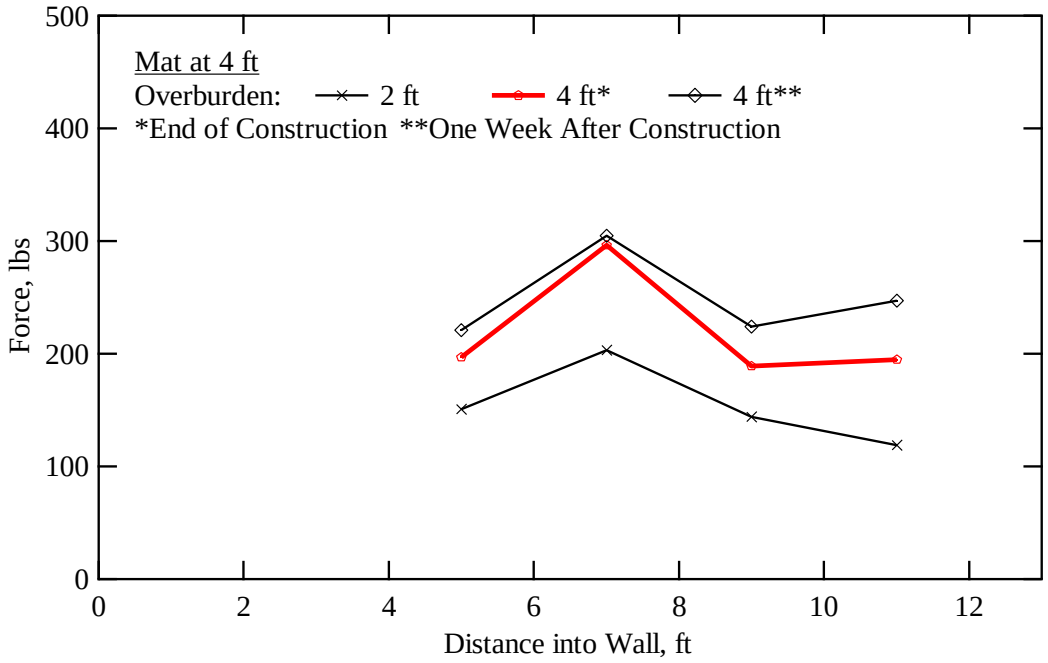

Figure 4.3 Tensile forces in crimped reinforcement mat 4 ft above base of the wall

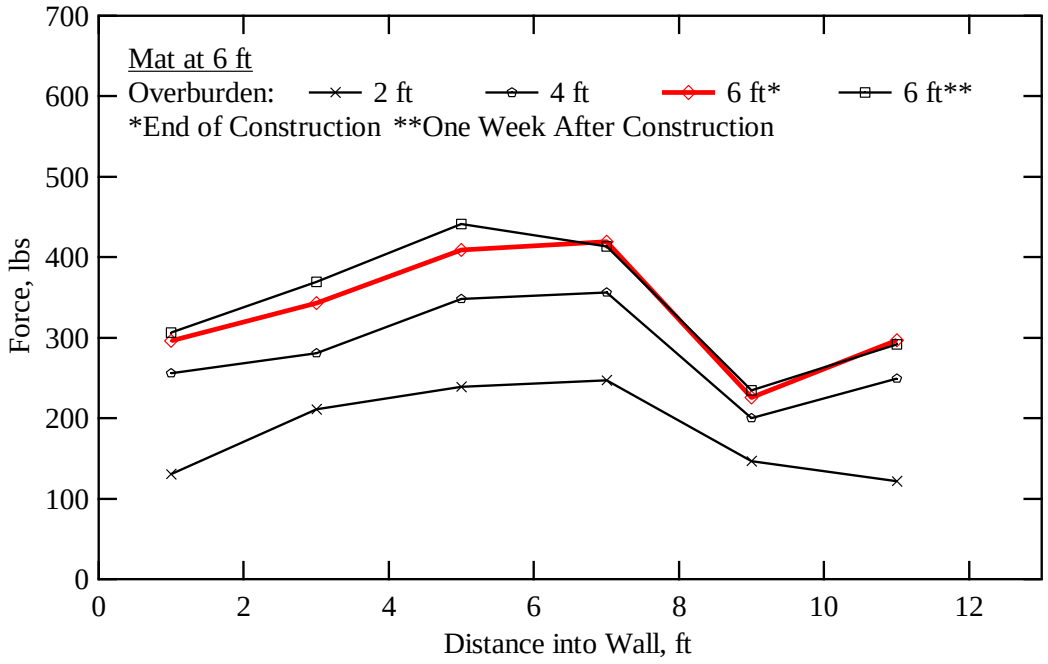

Figure 4.4 Tensile forces in crimped reinforcement mat 6 ft above base of the wall

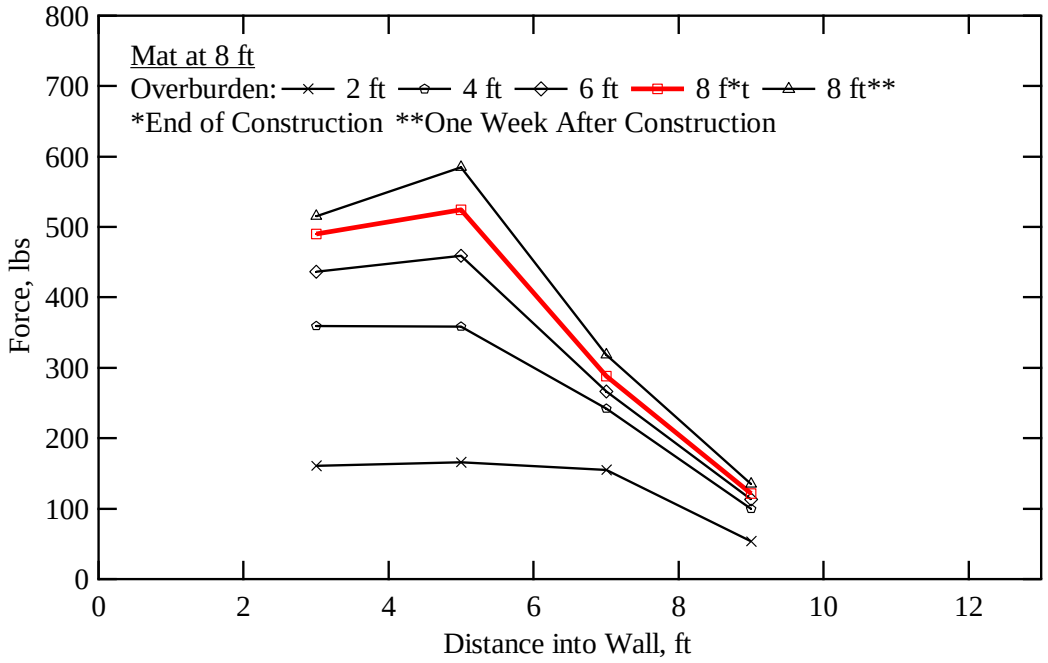

Figure 4.5 Tensile forces in crimped reinforcement mat 8 ft above base of the wall

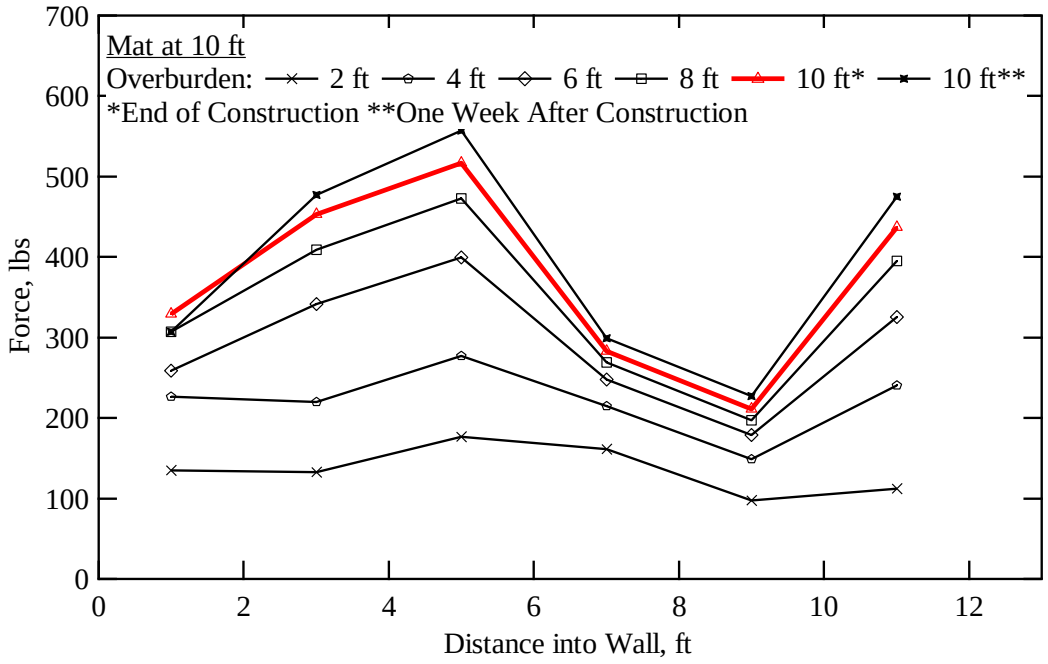

Figure 4.6 Tensile forces in crimped reinforcement mat 10 ft above base of the wall

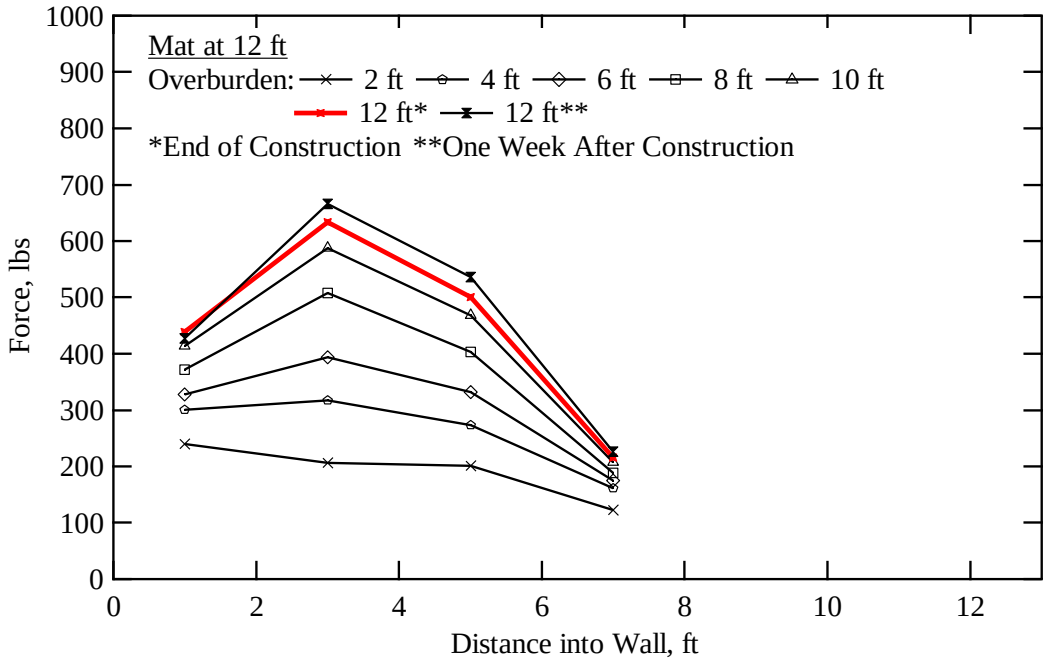

Figure 4.7 Tensile forces in crimped reinforcement mat 12 ft above base of the wall

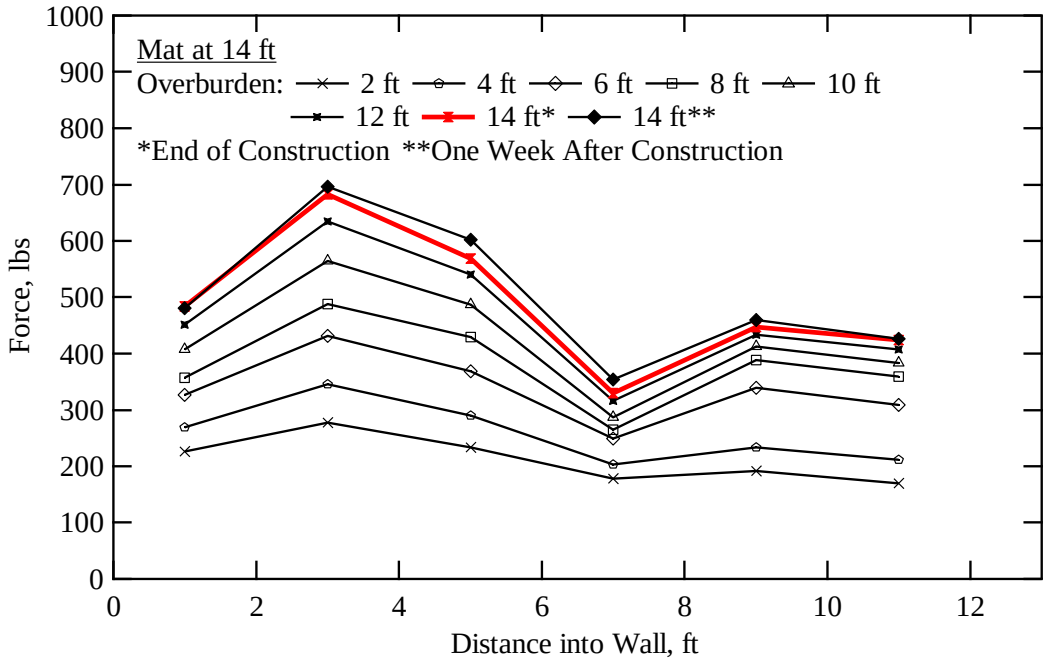

Figure 4.8 Tensile forces in crimped reinforcement mat 14 ft above base of the wall

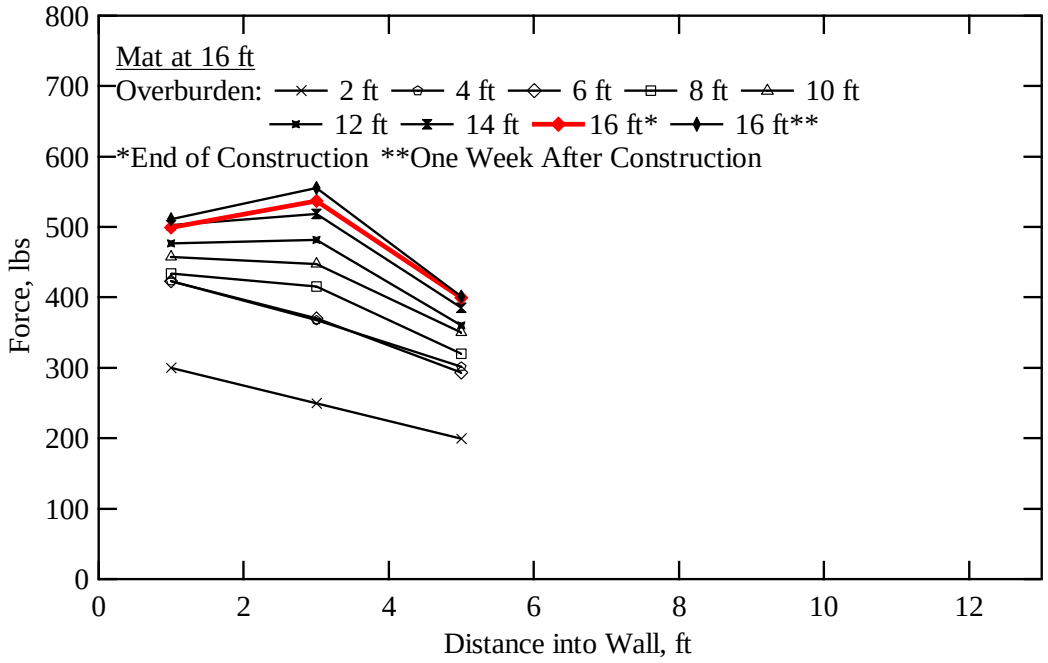

Figure 4.9 Tensile forces in crimped reinforcement mat 16 ft above base of the wall

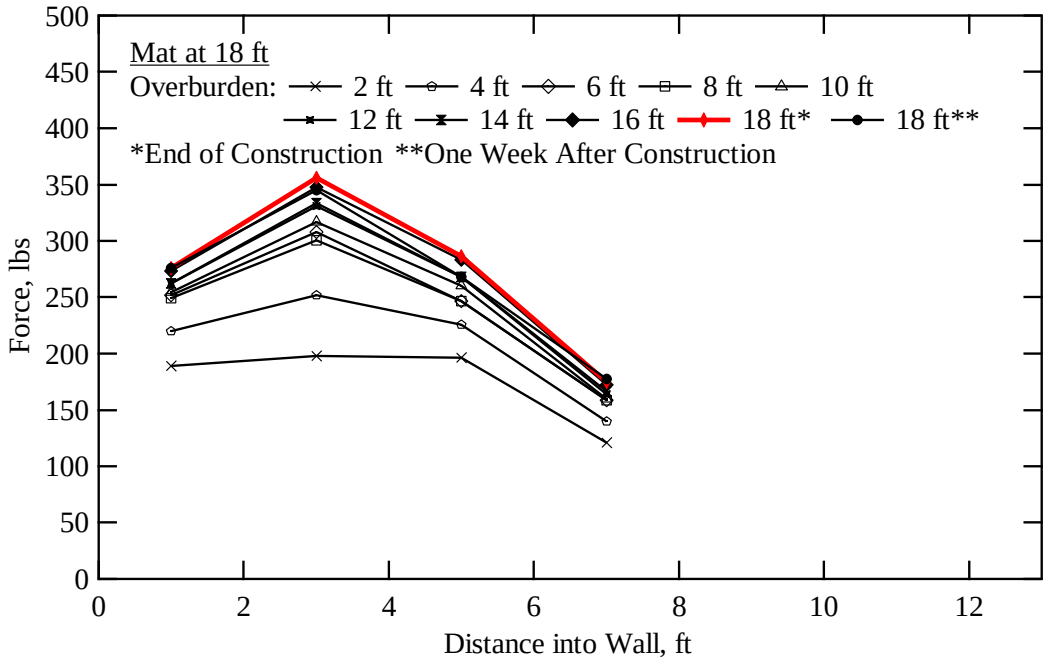

Figure 4.10 Tensile forces in crimped reinforcement mat 18 ft above base of the wall

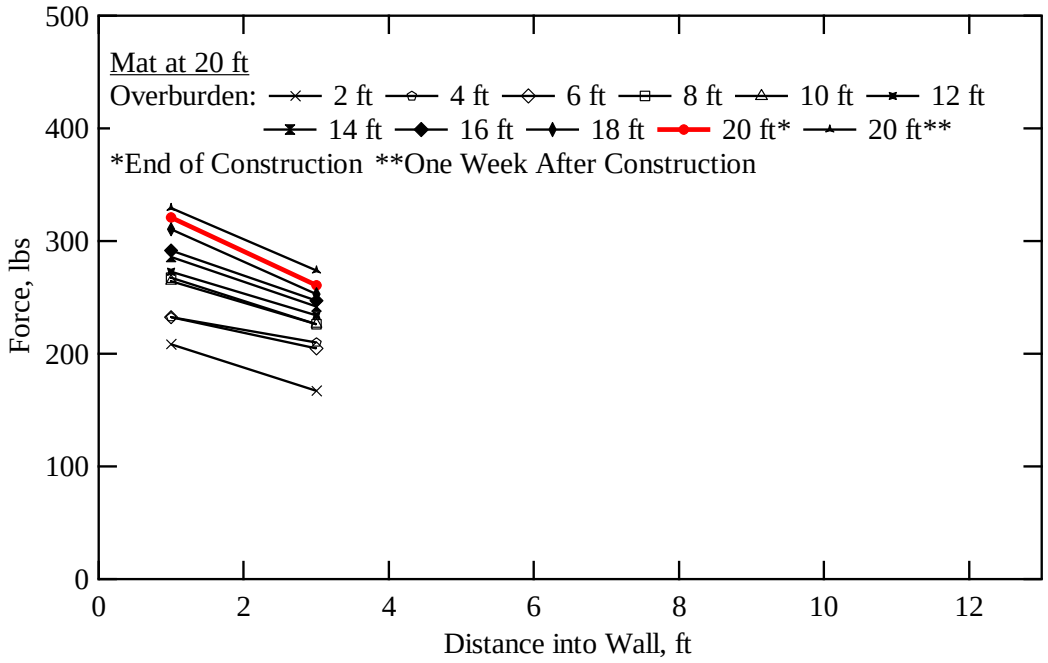

Figure 4.11 Tensile forces in crimped reinforcement mat 20 ft above base of the wall

4.4 Face Deflections

Figure 4.12 shows the recorded deformations at the face of the wall as the wall was constructed and also one week after construction had finished. It can be seen that the reinforcement allows for extension and meets the guidelines established by previous research that an active loading condition has been achieved if the deformations at the face of the wall are in the range of 0.2% to 0.5% of the height of the wall (0.25" to 0.5") (Bonaparte and Schmertmann, 1988). This wall goes beyond the range given, however it does not eliminate the fact that it has reached its active state.

The excessive deformation at the face is likely due to constructability issues as the wall was built. For the first three to four lifts, the equipment operator was using the bucket of the excavator to push soil into the face of the wall. It was observed that in

doing so, excessive deformation occurred upon placement of the bucket. Simply, the compaction effort near the face of the wall during construction was excessive and should be restricted to lightweight manual compaction equipment rather than heavy machinery.

Because the compaction of the lifts generated so much initial deflection, the plot presented for the face deflections represents the recorded measurements one lift after initial measurements were taken. This was done to remove the bias of compaction methods used in construction.

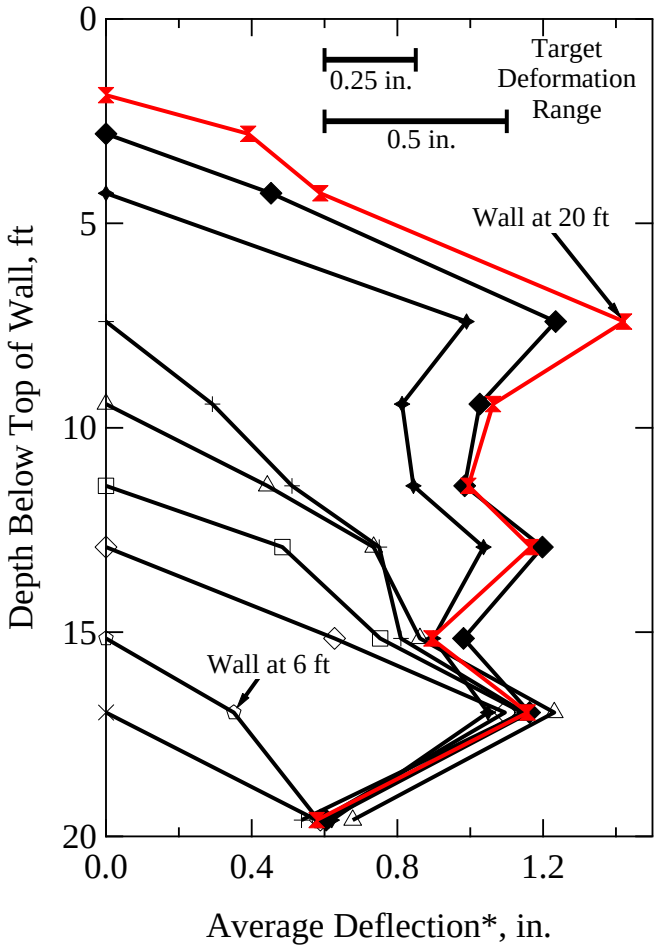

Figure 4.12 Deflection measurements of the wall face.
*Deflection measurements are relative to one lift after initial readings.

4.5 K Values

The K values were back calculated using the tension values for the wall. Figure 4.13 shows the calculated K values for the wall as it was constructed and as it reached its full height and is compared to an inextensible steel wire mat reinforcement and to an active state extensible reinforcement corresponding to a friction angle of 40°.

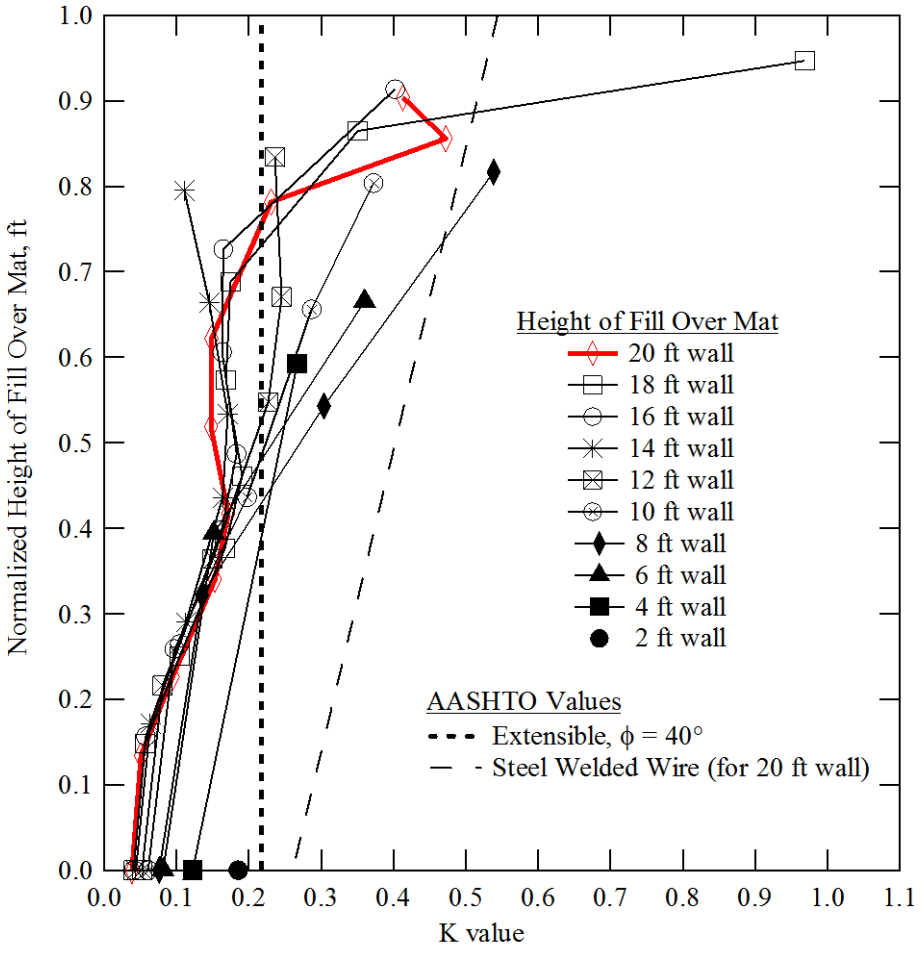

Figure 4.13 Back calculated K values as the wall was constructed

The K value represents the behavior of the wall, whether it is in some at-rest condition or if it is in its active condition. It can be seen in Figure 4.13 that the wall is not behaving in a typical inextensible fashion, but is rather tending to behave more as an extensible material. The active earth pressure coefficient was calculated by rearranging Equation 2.3 to solve for k_a.

4.6 Locus of Maximum Tension

The locus of maximum tension also helped reveal the behavior of the wall. Figure 4.14 shows the locus of maximum tension in the wall and how it progressed as the wall was built. It can be seen in Figure 4.14 that as the height of the wall continues to grow, the more the tension profile trends toward extensible behavior. The first four lifts were left out of this chart for clarification purposes only.

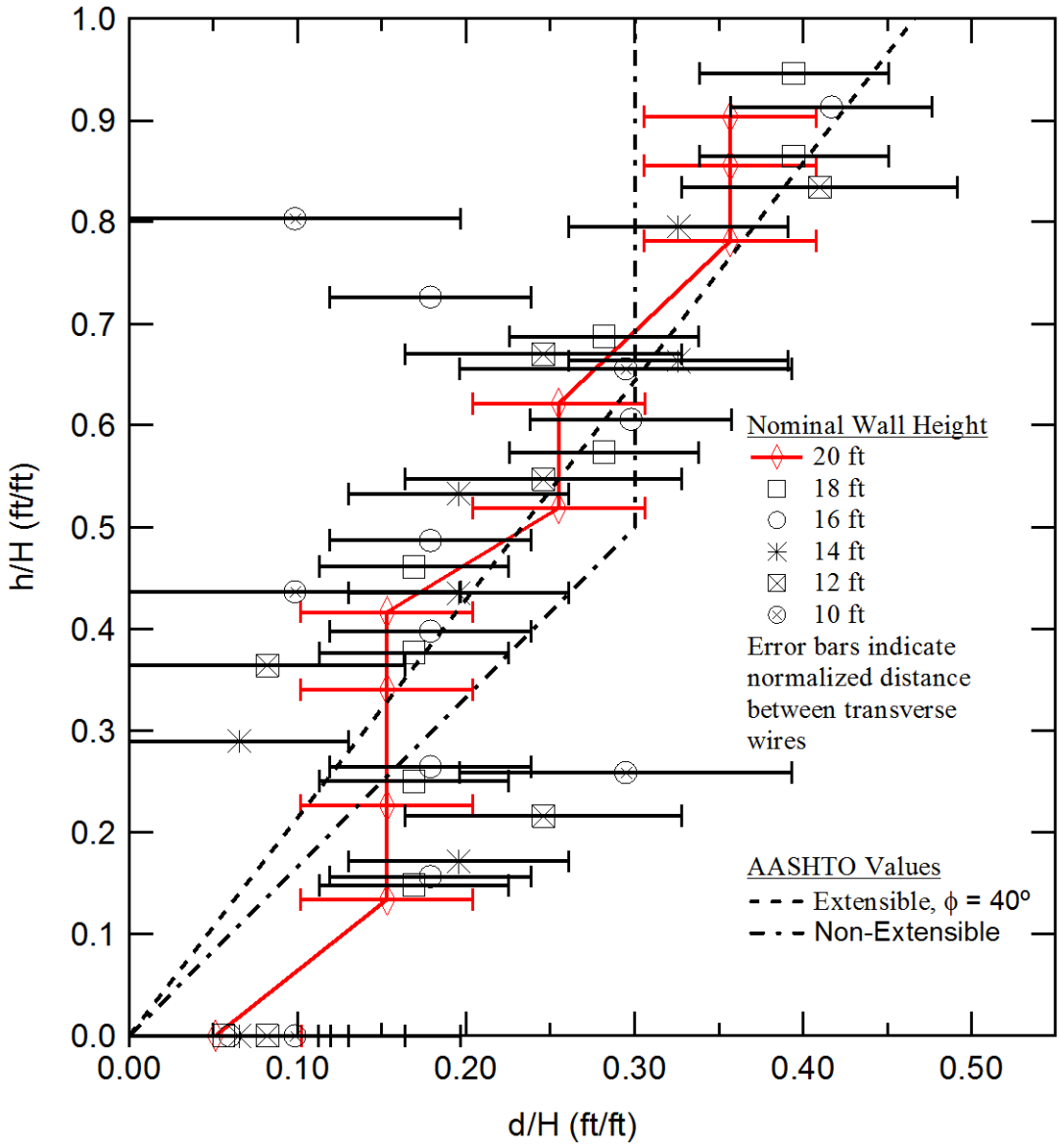

Figure 4.14 Locus of maximum tension comparison

CHAPTER 5

COMPARISONS BETWEEN DESIGN METHODS

5.1 Overview

One of the purposes of this paper was not just to analyze a new type of reinforcement, but also to critique the traditional AASHTO LRFD method beside the newer K-Stiffness method. This chapter compares the observed findings presented in Chapter 4 with what would be expected from both design methods.

5.2 Observations Compared with AASHTO LRFD Method

Figure 5.1 presents a comparison of observed maximum tension in the wall compared to an extensible design by AASHTO LRFD specifications. To properly compare the numbers, it was required to calculate the tensions by force per foot of wall width. For this reason Figure 5.1 shows the recorded maximum tensions with units as kip/ft versus the depth below the top of the wall. Also shown in Figure 5.1 is the factored rupture capacity and factored pullout capacity of the reinforcement material.

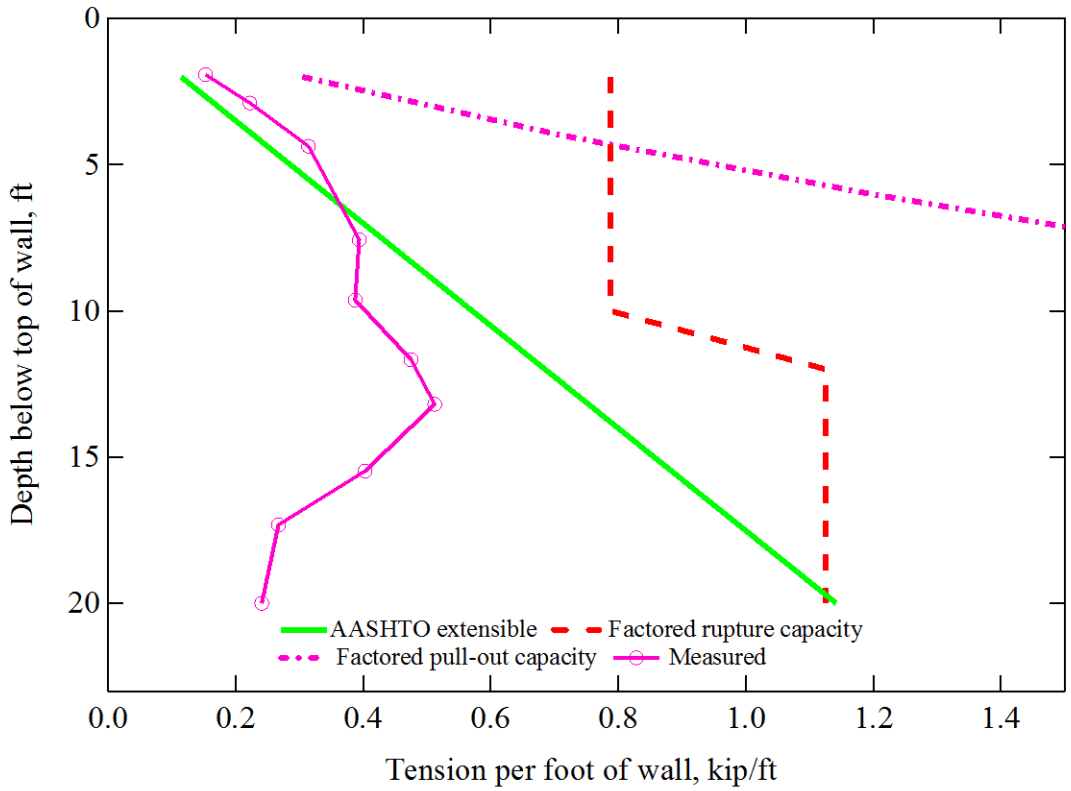

Figure 5.1 Observed tensions compared to AASHTO LRFD specifications

Figure 5.1 indicates the AASHTO design specifications greatly overestimate what is actually occurring in the bottom half of the crimped MSE wall. The top six feet of the wall was the exception. The top portion of the wall is typically governed by pullout resistance whereas the bottom portion of the wall is typically governed by rupture capacity.

5.3 Observations Compared to K-Stiffness Method

Figure 5.2 shows the comparisons of the observed behavior in the MSE wall compared to the K-Stiffness predicted behavior. It can be seen in Figure 5.2 that the K-Stiffness design method more accurately reflects the observed behavior of the MSE wall.

The AASHTO predicted behavior was added to the figure to show how the two design methods differ in their predictions.

The figure also shows the varying predictions of MSE walls by the type of reinforcement used. The predictions were calculated using the stiffness factors pulled from Figure 2.8 for the K-Stiffness plots shown, and the Load and Resistance Factors from Tables 2.1 and 2.2 for the AASHTO predicted plot. It can be seen that the lowest tensions are found in geosynthetic materials whereas the metallic types have higher values of tension. The crimped wire mats used in the wall were found to have an 85% decrease in stiffness than that of the non-crimped wire mats which corresponds to a 40% reduction of the tensions seen between the two. This places the new crimped wire reinforcement mats between the two traditional types of extensible and inextensible reinforcements, favoring the extensible materials. The compromise between the two materials was expected and is validated by the data collected as shown in Figure 5.2.

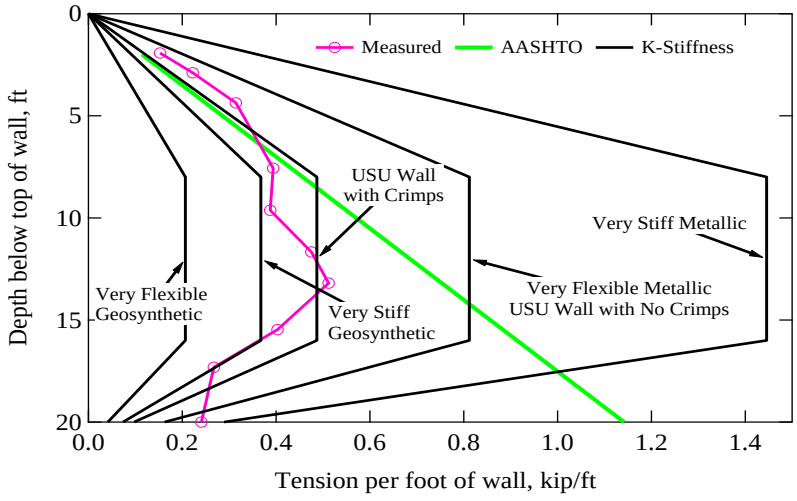

Figure 5.2 Comparison of varying types of reinforcement using K-Stiffness estimated values, expected AASHTO LRFD method, and measured tensions of crimped wire wall

CHAPTER 6

CONCLUSIONS AND FUTURE CONSIDERATIONS

6.1 Conclusion

This project successfully measured the tensions in a full scale 20 ft tall MSE wall, and provided excellent information in continuing research in the field of civil engineering and geotechnical engineering. It was found that the crimped steel wire reinforcement mats developed by Hilfiker Retaining Walls does work as expected. The crimped wire mats are compliant enough to achieve an active state in the MSE wall while retaining the material properties of the steel to keep it from creeping like a geosynthetic material. The evaluation of the K values, face deflections, and locus of maximum tension confirm an active state behavior. This will effectively lessen the design loads in the reinforcement material and will lessen the amount of steel required for design.

It was also found the AASHTO LRFD method for MSE walls greatly overestimates the observed behaviors when compared to the crimped welded wire mat reinforcements. Considering the design for this project assumed the new crimped wire reinforcement mats as a fully extensible product, this is significant. Much of the reinforcement material was eliminated in preliminary design by the assumption of a fully extensible material and yet it was found only 51% of the rupture capacity was used. The MSE wall is more accurately predicted by the K-Stiffness method developed by Allen and Bathurst (2003). This may be because Allen and Bathurst approach the design of MSE walls more as a shoring design such as a tie back wall or a braced excavation which takes into consideration friction at the base of the wall. The AASHTO design approaches

the MSE wall as a traditional gravity wall which does not consider friction at the base of the wall.

6.2 Future Considerations and Continuing Research

Future research with the crimped wire reinforcement mats should focus on establishing the material as a viable candidate for reinforcement selection in both short term and long term studies. Also, establishing the K-Stiffness method as an acceptable alternative design to the AASHTO LRFD method could encourage the production of MSE retaining walls for applicable sites.

For the industry to begin using this new type of reinforcement it will be necessary to conduct further studies that investigate the behavior of the semi-extensible wire mats. Preferably studies would be done on walls that are being put into production and permitted by the private owners to conduct research on the wall being built. This will encourage design variances which create dynamic settings that would be difficult to estimate in a pure academic setting. However, furthering controlled experiments according to AASHTO tolerances should still continue to be investigated in an academic setting to provide the necessary data to begin implementing the semi-extensible material in standard design practices. In short, more test walls need to be studied in controlled settings to establish design, as well as walls that are in service to establish a range of performance under varying conditions.

More test walls should be built to continue to compare the K-stiffness design methods to the AASHTO LRFD method. Case studies have found that the AASHTO design method does not accurately predict the behavior of MSE walls and that it

overestimates the loads that occur. The only way to change the standard design practices is to gather more data in more MSE walls and to provide a design alternative. Allen and Bathurst have done much already to challenge the AASHTO standard design practices by introducing the K-Stiffness design method. This design method has been accepted by the Washington Department of Transportation as an alternate design method but must conform to strict site qualifications. Awareness of the overestimation in design by practicing engineers will go a long way to challenge AASHTO design methods. Publishing test results in peer reviewed ASCE articles would provide a great opportunity to make the field of practicing engineers and researchers aware and interested.

Understandably, acceptance of the K-stiffness method as a standard design practice has been slow because of its empirical background. It was observed by this researcher that the design method seems to be similar to that of a braced excavation. It may be worth investigating a possible alternative design method for a MSE based on the mechanics of a braced excavation.

It would be interesting to see where the limits of the semi-extensible product are. To test the limits of the product, taller walls and walls with smaller wire diameters should be tested. It would be of specific worth to test the behavior of a taller MSE wall reinforced with the semi-extensible product in a controlled setting. A wall height of 30’ or 40’ should be tested to see if the behavior continues to act as an active case.

Also, long term studies of MSE walls constructed with the semi-extensible wire mats would be required to establish the product as a viable option in design. It is most likely that the long term testing would need to be done in walls that will be in service.

REFERENCES

AASHTO. (2010). *AASHTO LRFD bridge design specifications* (5th ed.). American Association of State Highway and Transportation Officials, Washington, DC.

Allen, T. M., and Bathurst, R. J. (2003). *Prediction of reinforcement loads in reinforced soil walls*. Washington State Department of Transportation, Seattle, WA.

Bonaparte, R., and Schmertmann, G. (1988). "Reinforcement extensibility in reinforced soil wall design." *The application of polymetric reinforcement in soil retaining structures,* P. Jarret & A. McGown, eds., Kluwer Academic Publishers, Norwell, MA. 409-457.

Suncar, O. (2010). "Pullout and tensile behavior of crimped steel reinforcement for MSE walls." M.S. Thesis, Utah State University, Logan, UT.

Yannas, S. F. (1985). "Corrosion susceptibility of internally reinforced soil-retaining walls." *FHWA RD-83-105.* Federal Highway Administration, U.S. Department of Transportation, Washington, DC.